CARINI APARECIDA LELIS

INTERAÇÕES INTERMOLECULARES ENTRE PROTEÍNAS DO SORO DO LEITE E MOLÉCULAS DE INTERESSE NA ÁREA DE ALIMENTOS

Tese apresentada à Universidade Federal de Viçosa, como parte das exigências do Programa de Pós-Graduação em Ciência e Tecnologia de Alimentos, para obtenção do título de *Doctor Scientiae.*

VIÇOSA
MINAS GERAIS - BRASIL
2019

Ficha catalográfica preparada pela Biblioteca Central da Universidade Federal de Viçosa - Câmpus Viçosa

T
L541i
2019

Lelis, Carini Aparecida, 1989-
Interações intermoleculares entre proteínas do soro do leite e moléculas de interesse na área de alimentos / Carini Aparecida Lelis. – Viçosa, MG, 2019.
xii, 51 f. : il. (algumas color.) ; 29 cm.

Orientador: Ana Clarissa dos Santos Pires.
Tese (doutorado) - Universidade Federal de Viçosa.
Inclui bibliografia.

1. Curcumina. 2. Enrofloxacina. 3. Soro do leite - Proteínas. 4. Forças intermoleculares. I. Universidade Federal de Viçosa. Departamento de Tecnologia de Alimentos. Programa de Pós-Graduação em Ciência e Tecnologia de Alimentos. II. Título.

CDD 22. ed. 667.26

CARINI APARECIDA LELIS

INTERAÇÕES INTERMOLECULARES ENTRE PROTEÍNAS DO SORO DO LEITE E MOLÉCULAS DE INTERESSE NA ÁREA DE ALIMENTOS

Tese apresentada à Universidade Federal de Viçosa, como parte das exigências do Programa de Pós-Graduação em Ciência e Tecnologia de Alimentos, para obtenção do título de *Doctor Scientiae.*

APROVADA: 28 de fevereiro de 2019.

Manoela Maciel dos Santos Dias

Tiago Antônio de Oliveira Mendes

Marcia Cristina Teixeira Ribeiro Vidigal

Luis Henrique Mendes da Silva
(Coorientador)

Ana Clarissa dos Santos Pires
(Orientadora)

AGRADECIMENTOS

A Deus, pela oportunidade oferecida, pelo conforto nos momentos de angustia e por me iluminar nos momentos de escuridão.

Aos meus pais, José e Lúcia, aos meus irmãos Camila e Mateus por todo apoio, paciência, amizade, amor e incentivo em mais essa etapa.

Á Universidade Federal de Viçosa e ao Departamento de Tecnologia de Alimentos, pela oportunidade de realização do curso.

A Coordenação de Aperfeiçoamento de Pessoal de Nível Superior, pela concessão da bolsa de estudo. A CNPq, FAPEMIG e Vale S. A. pelo financiamento do projeto.

A minha orientadora, professora Ana Clarissa dos Santos Pires, pela orientação, ensinamentos, apoio, diálogo, incentivo e confiança proporcionados.

Ao meu co-orientador, professor Luís Henrique Mendes da Silva, pelos ensinamentos, colaboração e assistência na realização desse trabalho. Pela disponibilização do uso de equipamentos do seu laboratório sempre que necessário.

Ao meu co-orientador, professor Nélio José de Andrade pelos ensinamentos, confiança e parceria.

Aos professores Márcia Cristina Teixeira Ribeiro Vidigal, Manoela Maciel dos Santos Dias e Tiago Antônio de Oliveira Mendes pela participação na banca de defesa.

Aos amigos do THERMA, pela amizade, pelo auxílio no desenvolvimento do trabalho e por me engrandecer como pessoa e profissional.

A todos do QUIVECOM pela ajuda na realização de analises do experimento.

A todos os colegas da Pós-Graduação pela agradável convivência e incentivos.

A todos, que de alguma forma, foram importantes para a realização deste trabalho.

BIOGRAFIA

Carini Aparecida Lelis, filha de José Francisco de Oliveira Lelis e Lúcia Eunice do Carmo Lelis, nasceu em Viçosa, Minas Gerais, em 03 de abril de 1989.

Em março de 2008, ingressou no curso de Ciência e Tecnologia de Laticínios na Universidade Federal de Viçosa (UFV), graduando-se em novembro de 2012.

Em abril de 2013 iniciou o mestrado no Programa de Pós-Graduação em Ciência e Tecnologia de Alimentos, na Universidade Federal de Viçosa, obtendo seu título em fevereiro de 2015.

Em março de 2015 iniciou o doutorado no Programa de Pós-Graduação em Ciência e Tecnologia de Alimentos, na Universidade Federal de Viçosa, submetendo-se à defesa de tese em fevereiro de 2019.

SUMÁRIO

LISTA DE FIGURAS

Capítulo 1

Capítulo 2

LISTA DE TABELAS

Capítulo 1

Capítulo 2

RESUMO

LELIS, Carini Aparecida, D.Sc., Universidade Federal de Viçosa, fevereiro de 2019. **Interações intermoleculares entre proteínas do leite e moléculas de interesse na área de alimentos**. Orientadora: Ana Clarissa dos Santos Pires. Coorientadores: Luis Henrique Mendes da Silva e Nélio José de Andrade.

As proteínas do leite têm sido alvo de estudos como estruturas para veiculação de pequenas moléculas como, drogas lícitas, compostos bioativos, corantes, etc. Estas proteínas apresentam em sua estrutura sítios capazes de interagir com compostos hidrofóbicos e assim veiculá-los. A ENRO é um antibiótico utilizado no tratamento de vacas com mastite e, quando boas práticas agropecuárias não são realizadas, resíduos de antibióticos são encontrados no leite. A CUR é um corante natural, utilizado na indústria de alimentos, que apresenta propriedades bioativas. Várias moléculas, inclusive proteínas, tem sido estudado para interagir com a CUR e assim transporta-la. No entanto, não há estudos na literatura propondo a bLF como molécula de transporte para a CUR. O presente trabalho teve como objetivo estudar a nível molecular os mecanismos envolvidos na interação entre: curcumina (CUR) e lactoferrina (bLF) e, enrofloxacina (ENRO) e albumina do soro bovino (BSA), em diferentes condições de temperatura e em pH fisiológico. Para o estudo de interação entre bLF e CUR foram utilizadas técnicas sensíveis e eficazes como fluorescência e a ressonância plasmônica de superfície (SPR). No estudo de interação entre BSA e ENRO foi utilizado a espectroscopia de fluorescência. Resultados de fluorescência mostraram que a intensidade de fluorescência da bLF diminuiu à medida que as concentrações de CUR aumentaram. O mecanismo de extinção da fluorescência foi classificado como estático, havendo portanto, a formação de complexos entre bLF e CUR nas condições termodinâmicas estudadas. Além disso, a variação de energia livre de Gibbs de formação de complexo foi negativa, sendo regida pela entropia. A análise de SPR também demonstrou a ocorrência de formação de complexos entre bLF e CUR. No entanto, em baixas temperaturas (285.15 K a 293.15 K) o processo foi regido pela entropia, já em temperaturas maiores (297.15 K a 301.15 K) foi regido pela entalpia. Adicionalmente, verificou-se que as novas interações formadas com a formação do complexo apresentaram menor capacidade de transferência de energia nas formas potencial do que quando as moléculas estavam livres. O estudo cinético de

formação de complexo entre bLF e CUR mostrou que a energia de ativação para a associação e dissociação do complexo (bLF-CUR) aumentou com o aumento da temperatura. Em baixas temperaturas, CUR demonstrou interagir preferencialmente na superfície da bLF, já em temperaturas mais elevadas a CUR se insere no interior da proteína. Também foi verificado a ocorrência do fenômeno de compensação entalpia-entropia, estando relacionado principalmente a dessolvatação e a mudanças conformacionais no local de interação. Para o estudo de interação entre BSA e ENRO, foi utilizado a espectroscopia de fluorescência, baseando-se na capacidade da ENRO em emitir fluorescência. No estudo verificou-se que ENRO se ligar preferencialmente no subdomínio IIA (sitio I) da BSA, sendo o processo de interação exotérmico. O complexo formado demonstrou ser mais estável em baixas temperaturas. Também foi verificado que no processo de formação do complexo BSA-ENRO houve a compensação entalpico-entropico e, as novas interações formadas com a formação do complexo (BSA-ENRO) apresentaram maior capacidade de transferência de energia para as formas potenciais que as interações que ocorrem quando as moléculas estão livres, ao contrário do que foi observado para bLF e CUR. Este estudo contribui para o conhecimento em nível molecular da interação entre proteínas do leite e moléculas de interesse na área de alimentos, em diferentes condições de temperatura e pH fisiológico, sendo um guia útil para a otimização da utilização de proteínas do soro como carreadoras.

ABSTRACT

LELIS, Carini Aparecida, D.Sc., Universidade Federal de Viçosa, February, 2019. **Intermolecular interactions between milk proteins and molecules of interest in the food area.** Adviser: Ana Clarissa dos Santos Pires. Co-advisers: Luis Henrique Mendes da Silva and Nélio José de Andrade.

Milk proteins have been studied for the transport of small molecules, such as pharmaceuticals, bioactive compounds, dyes, etc. These proteins have in their structure sites capable of interacting with hydrophobic compounds and thus carry them. The objective of this study was to study the molecular mechanisms involved in the interaction between curcumin (CUR) (bioactive compound) and lactoferrin (bLF) and enrofloxacin (ENRO) and bovine serum albumin (antibiotic used in the treatment of cows with mastitis) under different temperature conditions and at physiological pH. For the interaction study between bLF and CUR, sensitive and efficient techniques were used, such as fluorescence and surface plasmon resonance (SPR). Fluorescence results showed that the fluorescence intensity of bLF decreased with increasing concentrations of CUR. The fluorescence quenching mechanism was classified as static, showing the occurrence of complex formation between bLF and CUR under the thermodynamic conditions studied. In addition, the Gibbs free energy variation of the complexation was negative, being governed by entropy. SPR analysis also demonstrated the occurrence of complex formation between bLF and CUR. However, at low temperatures (285.15 K to 293.15 K) the process was governed by entropy, and at higher temperatures (297.15 K at 301.15 K) was governed by enthalpy. In addition, it was found that the complex formed had lower energy transfer capacity in the potential forms than the free molecules. The kinetic study of complex formation between bLF and CUR showed that the activation energy for association and dissociation of the complex (bLF-CUR) increased with increasing temperature. At low temperatures, the CUR showed to interact preferentially on the surface of the bLF, already at higher temperatures, the CUR penetrates inside the protein. It was also verified the occurrence of the enthalpy-entropy compensation phenomenon, namely related to the desolvation and to the conformational changes in the interaction site. for the interaction study between BSA and ENRO, fluorescence spectroscopy was used, based on ENRO's ability to emit fluorescence. In the study verified that the mechanism of

extinction of the fluorescence was static, occurring the formation of BSA-ENRO complex. ENRO demonstrated to bind preferentially to the subdomain IIA (site I) of the BSA, the interaction process being exothermic. the complex has been shown to be more stable at low temperatures. It was also verified that in the process of formation of the BSA-ENRO complex there was the enthalpy-entropic compensation and the formed complex (BSA-ENRO) presented greater capacity of transference of energy to the potential forms than the free molecules, unlike which was observed for bLF and CUR. This study contributes to the knowledge, at the molecular level, of the interaction between milk proteins and molecules of interest in the food area under different temperature conditions and physiological pH, being a useful guide for the optimization of the use of whey proteins as carriers.

INTRODUÇÃO GERAL

O leite bovino contém cerca de 3,5% (m/m) de proteínas que, além de fornecerem aminoácidos, são veículos naturais de micronutrientes essenciais, assim como componentes do sistema imune. As proteínas encontradas no leite são moléculas de custo relativamente baixo, alta disponibilidade, são reconhecidas como seguras, apresentam alto valor nutricional e são capazes de interagir com pequenas moléculas, principalmente moléculas hidrofóbicas, e assim veiculá-las. Essas características tem despertado o interesse da indústria de alimentos e farmacêutica para a utilização dessas proteínas no transporte de diversas moléculas.

As proteínas do leite são divididas em duas frações principais, as caseínas e as proteínas do soro. As proteínas do soro constituem um grupo bastante diversificados de proteínas com características estruturais e funcionais bem diferentes. Entre as proteínas do soro pode-se destacar a albumina do soro bovino (BSA) e a lactoferrina. A BSA é o principal transportador das mais variadas moléculas no organismo, seja moléculas de caráter hidrofóbico ou hidrofílico. A lactoferrina é uma proteína que apresenta em sua estrutura íons de ferro ligados, e apresentam várias funções fisiológicas importantes. Essas proteínas apresentam vários sítios de ligação com diferentes afinidades, podendo atuar no transporte de diferentes moléculas.

Ao interagir com pequenas moléculas, chamadas de ligantes, as proteínas do soro podem aumentar a solubilidade dos ligantes hidrofóbicos em meios aquosos, aumentar a biodisponibilidade, modular a entrega de drogas e compostos bioativos no organismo, além de proteger essas moléculas frente a condições do meio como, temperatura, luz, oxigênio, etc.

A CUR é um composto bioativo em que sua utilização em alimentos é limitada, uma vez que este bioativo é solúvel em óleo, apresenta pouca estabilidade contra o calor, luz e oxigênio, bem como baixa solubilidade. Dessa forma, sua aplicação em soluções aquosas possui baixa viabilidade técnica. A ENRO, um antibiótico utilizado no tratamento de animais com mastite, também é uma molécula com baixa solubilidade e molhabilidade em água, o que leva a dificuldades no desenvolvimento de formulações farmacêuticas.

A determinação dos parâmetros termodinâmicos e cinéticos de interação entre proteínas do soro e compostos de interesse (tipos de interações, estequiometria de formação do complexo, constante de interação, sítios de interação, constante cinética de associação e dissociação, energia de ativação do complexo ativado, capacidade calorifica, etc) é essencial para o melhor entendimento dos mecanismos de interação,

que são úteis para que as indústrias possam melhorar o desenvolvimento de sistemas de entrega.

Diante disso, a realização de pesquisas que visam entender as interações entre as proteínas do soro e moléculas de interesse pode contribuir para otimizar o transporte das mesmas. O transporte de drogas no sangue, assim como sua liberação, é de extrema importância do ponto de vista da farmacocinética. Já nos alimentos, o transporte de moléculas como os compostos bioativos pode melhorar as características sensoriais dos alimentos, manter propriedades funcionais e otimizar a utilização destes compostos. Com isso, o objetivo do nosso trabalho foi estudar a interação entre proteínas do soro de leite (bLF e BSA) e compostos de interesse na área de alimentos (CUR e ENRO), fornecendo informações uteis para a otimização da utilização dessa proteínas no transporte de moléculas como CUR e ENRO.

Capítulo 1: Lactoferrin-curcumin binding: a thermodynamic, and kinetic study of an important biofunctional complex

Abstract

An understanding of the thermodynamics and kinetics of the interaction between bovine lactoferrin (bLF) and curcumin (CUR) is needed for the application of this system to food and pharmaceutical formulations. We used fluorescence spectroscopy (FS) and surface plasmon resonance (SPR) to study the formation of the bLF-CUR complex. The fluorescence spectroscopy results showed positive values of standard enthalpy and entropy changes ($\Delta H°$ = 66.5 kJ·mol^{-1} and $T\Delta S°$ = 90.7 to 94.7 kJ·mol^{-1}), indicating that hydrophobic interactions are the main forces contributing to bLF-CUR binding. The $\Delta H°$ values obtained by SPR were lower ($\Delta H°$ = 42.83 to -35.86 kJ·mol^{-1}), suggesting that the interactions that occur far from the Trp residues release more energy. $\Delta Cp°$ value was negative, indicating that the bLF-CUR complex has less ability to transfer heat energy to the potential form than the free bLF and CUR molecules. Through the energy parameters it was possible to propose that at low temperature CUR interacted at bLF interface, however with the increase in the temperature the bioactive molecule penetrates into the inner of the protein. In both studies of thermodynamic and kinetics parameters obtained by SPR, the occurrence of the enthalpy-entropy compensation (EEC) phenomenon was verified. Thus, this work show a complete thermodynamic and kinetic characterization of the formation of the bLF-CUR complex, providing important information for technological applications of this important biofunctional complex.

Keywords: lactoferrin; curcumin; fluorescence; surface plasmon resonance

1. Introduction

Bovine lactoferrin (bLF) is a member of the transferrin family and is composed of 692 amino acids folded into two homologous globular lobes connected by turn helix and each lobe is formed by two domains connected by Fe^{3+} ions. bLF is found in cow milk, mucosal secretions, tears, saliva, blood (Croguennec, Li, Phelebon, Garnier-Lambrouin, & Gésan-Guiziou, 2012; Farnaud & Evans, 2003) and exhibits many important biological functions as an antioxidant, anticancer agent, and carrier of iron and different bioactive compounds [1,6–9]. Because of these properties, bLF has been increasingly used in different food products (Bokkhim et al., 2015), such as fortified yoghurts, infant formulae, and dietary supplements (Wakabayashi et al., 2006; Tomita et al., 2009). It has been intensively studied, and these studies have shown that bLF has potential to carry different bioactive compounds in food, as for exemple: (−)-epigallocatechin-3-gallate (EGCG) (Yang et al., 2014) and rosmarinic acid (Ferraro et al., 2015).

As example of bioactive compounds is curcumin (CUR), also known as diferuloylmethane [15], ¹⁵is a hydrophobic polyphenol extracted from turmeric. Studies have shown that CUR has potential as an antioxidant [5,16], anti-inflammatory and antitumor [4,17,18], as well as being a regulator of many biological processes [19]. However, CUR is almost insoluble in water (solubility = 0.6 μg/mL)[20] at acidic and neutral pH, which limits its bioavailability (Maiti et al., 2007; Wang et al., 2008). Moreover, CUR is sensitive to oxygen, light, and high temperatures [23].

Aiming to overcome these limitations, researchers have investigated different carriers for CUR. For example, Mangolim et al. (2014) showed important evidence of CUR–β-cyclodextrin (β-CD) inclusion complex formation. The occurrence of the interaction between CUR and β-CD intensified the color of the vanilla ice cream and produced a great sensory acceptance. Camel β-casein micelles demonstrated interact with CUR mainly via hydrophobic interactions, with a binding constant of 1.8×10^4 M^{-1}, at 298 K [25]. The complex formed between CUR and bovine serum albumin (BSA) analyzed by isothermal titration microcalorimetry, showed a binding constant of the

order of 10^5 M^{-1}, and the formation of the complex was entropically driven [26]. Thus, due to the presence of hydrophobic regions in their structure [27,28], the bLF may be a promising nanovehicle for CUR (Bollimpelli et al., 2016). However, there are no studies concerning the kinetics and thermodynamics of the interaction between bLF and CUR. Understanding the kinetics and thermodynamics of bLF-CUR binding is strategic because it can provide relevant information about the energetic e molecular dynamics of interaction between these molecules, enabling optimize their use in food products.

Fluorescence spectroscopy (FS) is one of the most used techniques to investigate the thermodynamic of protein–ligand binding because it is sensitivite, selective and rapid (Atrahimovich, et al. 2012). In addition, bLF presents in its structure 13 residues of tryptophan, which makes FS analysis strategic for the interaction study (Steijns and van Hooijdonk, 2000). However, for a more complete understanding of the dynamic processes of interaction between bLF and CUR, beyond to the thermodynamic parameters, a kinetic study of the interaction is required. Surface plasmon resonance (SPR) is a strategic technique able to analyze interaction between protein and analytes in a fast, sensitive and label-free way, detecting, at real-time, the binding events (Atale, Dyawanapelly, Jagtap, Jain, & Dandekar, 2019; Gombau et al., 2019; Schasfoort & Tudos, 2013). With the SPR, it is possible to determine thermodynamic and kinetic binding parameters in a single set of experiments.

Based on the potential of CUR and bLF as biofunctional compounds for food applications, this will be the first study to provide us with data on the thermodynamics and kinetics of interaction between bLF and CUR, thus helping to optimize the use of bLF as a carrier of CUR.

2. Material and Methods

2.1. Materials

Lactoferrin (>97% wt.), CUR (80% wt.), dibasic sodium phosphate ($NaHPO_4$), monohydrated sodium phosphate ($NaH_2PO_4 \cdot H_2O$), of analytical grade, were purchased from Sigma-Aldrich (St. Louis, MO, USA). Dimethyl sulfoxide (DMSO, C_2H_6OS), of analytical grade, was purchased from Neon Commercial Ltda (São Paulo, SP, Brazil). 3-(N,N-dimethylamino)propyl-N-ethylcarbodiimide (EDC) (> 99% wt), N-hydroxysuccinimide (NHS) (> 99% wt), sodium acetato (> 99% wt) and ethanolaminehydrochloride were purchased from General Electric Healthcare Company, (Sweden).

2.2. Fluorescence Experiments

Fluorescence spectra were obtained with an LS-55 spectrofluorimeter (Perkin-Elmer, USA) equipped with quartz cells (1.0 cm) and a thermostatic bath. Initially a solution of CUR 5×10^{-3} mol·L^{-1} in DMSO was prepared. From this solution was prepared the stock solution of CUR 1×10^{-4} mol·L^{-1}, in solution of bLF 3×10^{-6} mol·L^{-1}. For fluorescence measurements, 10 titrations of 50 µL of a stock solution of CUR (2.5 to 25 µM) in 2.0 mL of bLF solution (3.0×10^{-6} mol·L^{-1}) in a quartz cell and at pH 7.4 were used [34]. To minimize the effect of 10 titrations of CUR containing DMSO on the intrinsic protein fluorescence, we added 2% DMSO to the bLF solution in a quartz 3.0×10^{-6} mol·L^{-1}cell. bLF was excited at 295 nm and fluorescence emission spectra were then measured in the wavelength range of 296 to 450 nm, at five different temperatures (293.15, 296.15, 299.15, 303.15 e 306.15 K)

2.3. SPR experiments

The kinetics and thermodynamics of interaction between bLF and CUR were explored by SPR (Biocore X100 – GE Healthcare, Pittsburgh, PA, USA). Before analysis, bLF was immobilized on the CM5 sensor chip using a Biocore amine coupling

kit, according to the manufacturer's instructions. The carboxylic groups, formed when the sensor chip is docked in the instrument, was activated for 7 min with a 1:1 mixture of 0.1 mol.L^{-1} 3-(N,N-dimethylamino)propyl-N-ethylcarbodiimide (EDC) and 0.1 mol.L^{-1} N-hydroxysuccinimide (NHS) at a flow rate of 20 μL.min^{-1} and at 298 K. Then, a solution at 3.0×10^{-6} mol·L^{-1} of bLF in 10 mmol·L^{-1} of sodium acetate at pH 7.0 was injected for 7 min, resulting in a lower density bLF immobilization. A 7 min pulse of 1 mol L^{-1} ethanolaminehydrochloride, pH 8.5, was then injected to deactivate the excess hydroxysuccinimidyl groups on the surface that did not reacted with the protein.

The bLF-CUR binding experiments were carried out at pH 7.4 and temperatures that ranged from 285.15 to 301.15 K. The concentrations of the CUR solutions (30–100 μM) were prepared in flowing buffer sodium phosphate. In each binding experiment, the CUR solution at the required concentration was injected in order to increase colorant concentration over both sample (with immobilized bLF) and reference (without bLF) surfaces. The two-channel injection (sample and reference) was performed to correct for systematic noise and instrument drift. Between each bLF-CUR binding cycle, buffer was injected to determine the baseline.

The bLF image used to make a hypothetical description of the interaction sites of CUR for bLF were extracted from the Protein Data Bank (PDB ID: 1blf) (2.8 angstroms resolution) (http://www.pdb.org/pdb/home/home.do).

All experiments were carried out in triplicate and the relative errors were between 1 and 3 %. The results were expressed as mean ± standard deviation.

3. Results and Discussion

3.1. Fluorescence Measurements

Many proteins exhibits fluorescence mainly due to the Trp and Tyr residues [35]. The bLF has 13 Trp residues (Trp-8, Trp-16, Trp-22, Trp-24, Trp-125, Trp-138, Trp-268, Trp-347, Trp-361, Trp-448, Trp-467, Trp-549, and Trp-560) (Steijns and van Hooijdonk, 2000), which are accountable for the intrinsic fluorescence emission of the protein. The

binding between bLF and small molecules, such as CUR can quench bLF fluorescence. When it was excited at 295 nm, the resultant fluorescence maximum emission peak was about 335 nm (Figure 1). The addition of increasing CUR concentrations reduced the protein fluorescence intensity by 54%, indicating change around the region of tryptophan residues, which may be due to complex formation between bLF and CUR.

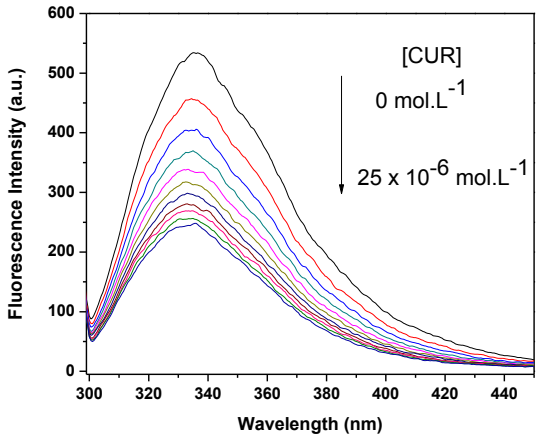

Figure 1. Fluorescence emission spectra of 3.0 μM bLF in the presence of 0, 2.5, 5.0, 7.5, 10.0, 12.5, 15.0, 17.5, 20.0, 22.5, 25.0 μM CURC at pH 7.4.

The fluorescence quenching data were studied using the Stern–Volmer equation (Eq. 1).

$$\frac{F_0}{F} = 1 + K_{sv}[Q] = 1 + K_q\tau_0[Q] \quad (1)$$

Here, F_0 and F are the fluorescence intensities of fluorophore before and after the addition of the quencher (CUR), respectively, [Q] is the quencher concentration (mol·L^{-1}), K_{sv} is the Stern-Volmer quenching constant, τ_0 is the average protein fluorescence lifetime in the absence of the quencher, and K_q is the biomolecular quenching constant. From the fluorescence intensities, it was possible to determine the values of K_{sv} by linear regression (F_0/F vs. [Q]).

The K_q values were found to be at least 50 times higher than the K_q values for biomolecules, i.e., 1.00×10^{10} L·mol^{-1}·s^{-1} [36]. This magnitude of K_q indicates that the

main fluorescence quenching mechanism is static, arising from complex formation between bLF and CUR (Silva *et al*., 2017; Lelis *et al.*, 2017; Nunes *et al*., 2017).

After the confirmation that the fluorescence quenching mechanism is predominantly static and assuming that the binding sites of the protein (bLF) for CUR are independent and with similar binding constants, the equilibrium between the free and bound CUR molecules at the bLF sites is given by the Stern–Volmer equation (Eq. 2).

$$\log\left(\frac{F_0-F}{F}\right) = \log K_b + n\log[Q_t] \quad (2)$$

Here, F_0 and F are the fluorescence intensities of bLF in the absence and the presence of CUR respectively, n is the number of binding sites, K_b is the binding constant, and $[Q_t]$ is the total CUR concentration.

The stoichiometry (n) and the binding constant (K_b) for complex formation were calculated applying the Eq. 2 to double logarithmic plot between log [(F_0 - F)/F] vs. log [Q] at five temperatures (Figure 2, Table 1). The n and K_b values were extracted from intercept and slope of this curve, respectively.

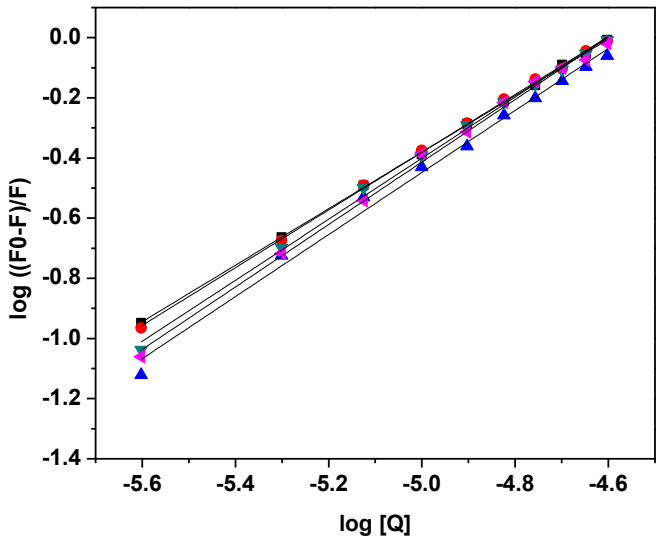

Figure 2. The plot of log[(F_0-F)/F] as a function of log [Q], being binding constant (K_b) the intercept and stoichiometry (n) the slope at pH 7.4.

The K_b values ranged from 2.07 a 6.68 x 10^4 $L \cdot mol^{-1}$, increasing about 3.3 times with increasing temperature, which indicates that the bLF-CUR complex is more stable at higher temperatures. The *n* values were close to 1 at all temperatures, suggesting that each avaible Trp site in bLF can interact with one CUR molecule. Other studies have found similar stoichiometries for CUR binding with different serum proteins, such as BSA [26], human serum albumin (HSA) (Ge *et al.*, 2014), α-lactoalbumin (α-la) (Mohammadi and Moeeni, 2015), and β-lactoglobulin (β-lg) (Mohammadi *et al.*, 2009). However, BSA, HSA, α-la, and β-lg contain 2, 1, 4 and 2 Trp residues, respectively, whereas bLF has 13 Trp residues, indicating that this protein can bind up to 13 CUR molecules, if all of Trp sites are available for interaction. This result provides important insights about the potential of bLF as a carrier for hydrophobic bioactive molecules.

The protein–ligand binding may consist of different interactions such as hydrogen bonds, electrostatic, hydrophobic, and van der Waals. To further elucidate the interactions between bLF and CUR, the thermodynamic parameters of complex formation ($\Delta G°$, $\Delta H°$, and $T\Delta S°$), were calculated following the approach: The standard Gibbs free energy change ($\Delta G°$) values were directly calculated from the K_b values at each temperature (Eq. 3); the standard enthalpy change ($\Delta H°$) value was determined by following the van't Hoff approach (Eq. 4) by the plotting of $\ln K_b$ versus 1/T, and the standard entropy change ($T\Delta S°$) was obtained using the fundamental Gibbs equation (Eq. 5), listed in Table 1.

$$\Delta G^0 = -RT ln K_b \quad (3)$$

$$\frac{lnK_{b2}}{lnK_{b1}} = -\frac{\Delta H^\circ}{R}\left(\frac{1}{T_2} - \frac{1}{T_1}\right) \quad (4)$$

$$T\Delta S° = \Delta H° - \Delta G^o \quad (5)$$

Here, *R* is the universal gas constant (8.3145 J·mol^{-1}·K^{-1}), *T* is the temperature (K), and *K* is the binding constant (L·mol^{-1}).

Table 1. Binding constants (K_b), the number of binding sites (n) and thermodynamic parameters of interaction between bLF and CUR at pH 7.4 at different temperatures.

T(K)	Kb [a]	n	ΔG° [b]	ΔH° [b]	TΔS° [b]
293.15	2.07±0.18	0.94±0.18	-24.2		90.7
296.15	2.60±0.19	0.96±0.19	-25.0		91.5
299.15	3.01±0.16	1.03±0.16	-25.6	66.5	92.1
303.15	4.72±0.32	1.01±0.32	-27.1		93.6
306.15	6.68±0.35	1.05±0.35	-28.2		94.7

The superscript letters representes the units: [a] (10^4 L·mol^{-1}) [b](kJ·mol^{-1}); R^2 = 0.99

The Δ*G*° values were found to be negative, indicating that the chemical equilibrium favored the formation of the bLF-CUR complex. The positive Δ*H*° and *T*Δ*S*° values indicate that the complex formation process was endothermic, being driven by the entropy increase, probably because of the hydrophobic interactions between bLF and CUR [42]. CUR has in its chemical structure hydrophobic groups such as benzene rings, which may interact with the hydrophobic side chains of the protein. Further, the release of water molecules from the solvation layer of both interacting molecules (bLF and CUR) resulted in an increase in the system entropy.

The enthalpic contribution (Δ*H*°) to bLF-CUR binding could be rationalized as a result of three molecular processes, i.e., desolvation of the bLF and CUR surfaces (ΔH_{des}), conformational change of the bLF interaction site ($\Delta H_{mud.conf}$), and the formation of the bLF-CUR interactions ($\Delta H_{bLF-CURC}$) (Eq. 6). The positive values of Δ*H*° show that the contribution of the endotermic processes, desolvation and denaturation, is higher than the process of the formation of the bLF-CUR interaction. Thus, the energy absorption process for the conformational change of the interaction site and the

release of water molecules from the solvating layer of bLF and CUR contributed more during the formation of the bLF-CUR complex.

$$\Delta H^0 = \Delta H_{des} + \Delta H_{mud.conf} + \Delta H_{bLF-CUR} \quad (6)$$

3.2. SPR results

While fluorescence spectroscopy is limited to analyze interactions, which occur close to the Trp residues on bLF, the SPR may be used as broader technique to explore bLF-CUR interaction. In addition, SPR allow us to obtain kinetic parameters associated to the formation of the bLF-CUR complex. These kinetic parameters are important because they can complement the thermodynamic data, providing information about the rate of complex association and dissociation [43].

In the sensogram obtained with the SPR (Figure 3) there are two main distinct regions in the sensorgram: region A where occurs simultaneously the complex association, and dissociation, prevailing the association process and region D, where the process of dissociation prevails.

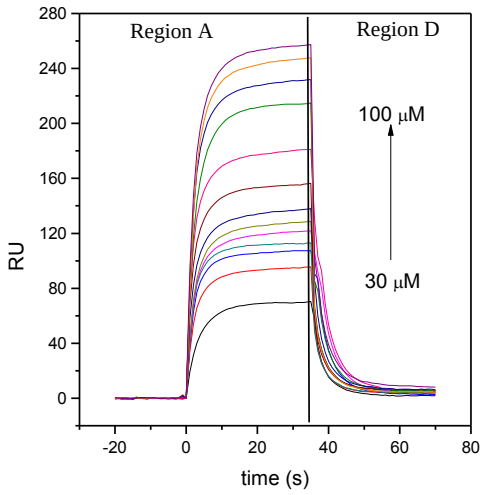

Figure 3. Sensograms (RU vs. time) for bovine lactoferrin -curcumin binding at 298 K and pH 7.4. The arrows indicates increasing CUR concentration (30-100 μM).

When the CUR solution flowed over the chip surface with immobilized-bLF, the resonance signal (resonance units - RU) along the time changed. From this it is possible to determine the kinetic rate constant of dissociation (k(d)), adjusting the data of the sensor to Eq. 7.

$$RU(t) = RU(t_m)\, e^{-k_d(t-t_m)} \quad (7)$$

where t_m is the time when dissociation process started and RU(t_m) is resonance in t_m.

The kinetic rate constant of association (k_a) was determined fitting the sensorgram data to Eq. 8 and then using Eq. 9. The k_a is the slope of the k_{obs} *vs.* $[CUR]$ plot.

$$RU(t) = RU_{max}(t_\infty)[1 - e^{-k_{obs}(t)}] \quad (8)$$

$$k_{obs} = k_a[CUR] + k_d \quad (9)$$

where $[RU(t)]$ is the SPR signal obtained in the sensorgram at time t, k_{obs} is the observed constant, and $[RU_{\max}(t_\infty)]$ is the SPR response at bLF saturation by CUR.

The k_a and k_d values are shown in Table 2.

Table 2. Kinetic rate constants for the association (k_a) and dissociation (k_d) of bovine lactoferrin-curcumin complex at pH 7.4.

T (K)	k_a (10^3 $M^{-1}s^{-1}$)	k_d (s^{-1})
285.15	1.23±0.06	0.31±0.01
289.15	1.23±0.05	0.26±0.01
293.15	1.27±0.07	0.24±0.01
297.15	1.37±0.09	0.25±0.01
298.15	1.46±0.10	0.27±0.01
301.15	1.70±0.12	0.37±0.01

The k_a and k_d values were of the order of 10^3 $M^{-1}s^{-1}$ and 10^{-1} s^{-1}, respectively, and they showed a second order polynomial dependence on temperature (Figure S1). Initially the values of k_a decreased and from 289 K increased. The same was observed

for k_d, with a minimum point at 292.5 K. This non-linear behavior indicates that both association of bLF and CUR to form bLF-CUR complex as well as its dissociation occurred in a multi-step process, involving conformational change of the protein. Moreover, the different behavior of k_a and k_d with temperature shows that the dissociation process is not reversible to the association, that is, changes occurring during the association to form the complex, are not completely undone by the dissociation of the complex and/or new changes during dissociation may occur.

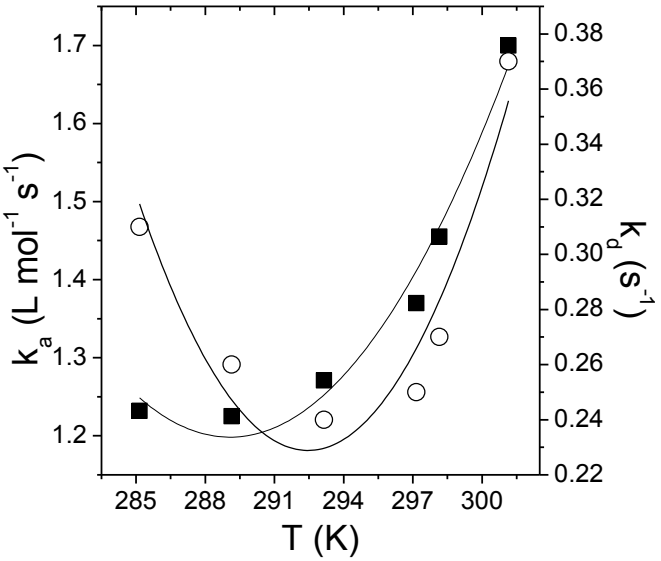

Figure S1 – Plots of k_a (■) and k_d (○) versus T for bLF-CUR interaction at pH 7.4. Polynomial equation for association process: $k_a = 0.003\ (T)^2 - 1.89\ (T) + 274.40$; $R^2 = 0.96$ and for dissociation process: $k_d = 0.001\ (T)^2 - 0.98\ (T) + 143.72$; $R^2 = 0.86$.

Hudson et al. (2018) found k_a and k_d values 10- and 2-fold higher, respectively, than those found by us for CUR interacting with BSA at pH 7.4 and 298.15 K (1.49 x 10^4 $M^{-1}s^{-1}$ and 6.77 x 10^{-1} s^{-1}) than those found for bLF-CUR. This difference can be related to the protein structure, size, and conformational changes induced by the interaction with CUR (Guo, Lu, Wang, & Brodelius, 2017).

The relationship between the kinetic rate constants yields the thermodynamic binding constant ($K_b = k_a/k_d$). Therefore, using the SPR kinetic experiment, the

thermodynamic parameters were also obtained (Eqs. 3-5), and they are presented in Table 3.

Table 3 Binding constants (K_b) and thermodynamic parameters (ΔG°, ΔH°, and TΔS°) of interaction and standard heat capacity change (ΔCp°) between bLF and CUR at pH 7.4 and different temperatures.

T (K)	k_b [a]	ΔG° [b]	ΔH° [b]	TΔS° [b]	ΔCp° [c]
285.15	3.97±0.16	-19.65±0.79	42.83±1.71	62.48±2.50	
289.15	4.71±0.23	-20.33±1.02	22.34±1.12	42.68±2.13	
293.15	5.30±0.16	-20.90±0.63	2.42±0.07	23.31±0.70	
297.15	5.48±0.28	-21.27±1.06	-16.98±0.04	4.29±0.21	-4.92
298.15	3.39±0.20	-21.30±1.28	-21.75±1.31	-0.45±0.03	
301.15	4.59±0.18	-21.11±0.84	-35.86±1.43	-14.75±0.59	

The superscript letters represents the units: [a] (10^3 L·mol^{-1}), [b] (KJ·mol^{-1}) and [c] (KJ·K^{-1}·mol^{-1}); R^2 = 0.99

The K_b values of bLF-CUR binding obtained by SPR ($K_{b\text{-}SPR}$) were of the order of 10^3 M^{-1}, showing to be 10 times lower than the K_b values found by fluorescence ($K_{b\text{-}FS}$). The K_b value is the product of the binding constants of each binding site for CUR in the protein ($K_b = K_{b1} \cdot K_{b2} \cdot \ldots \cdot K_{bn}$); thus, the SPR analysis detected all the available sites for in bLF interaction with CUR, including those not counted by FS, and these sites show lower K_b values, thus contributing to the reduce $K_{b\text{-}SPR}$ values.

Both techniques showed that when CUR interacts with bLF the Δ*G*° values were similar, -24.2 kJ.mol^{-1} and -20.90 kJ.mol^{-1} for FS and SPR, respectively, at 293.15 K. However, the values of ΔH° and TΔS° did not show exactly the same behavior in both techniques. For SPR, van 'Hoff approach showed a second order polynomial dependence of ΔH° in relation to the inverse of the temperature. The $\Delta H°_{SPR}$ values show that the process of interaction between bLF and CUR at low temperatures was endothermic, becoming exothermic with the increase in the temperature. The Eq. 6 can also be applied to evaluate the $\Delta H°_{SPR}$ values. At lower temperature, the $\Delta H°_{SPR}$ values

is positive because $|\Delta H_{des} + \Delta H_{ccs}| > |\Delta H_{bLF\text{-}CUR}|$. The CUR when interacting with the bLF can cause conformational changes in the protein, contributing to the positive values of ΔH°. In addition, when compared to higher temperatures, at lower temperature the water molecules are more structured around the hydrophobic regions the bLF e CUR, which demands more energy for desolvation. On the other hand, with the increase of the temperature, the water molecules are more unstructured, being $|\Delta H_{bLF\text{-}CUR}| > |\Delta H_{des} + \Delta H_{ccs}|$ and therefore, the ΔH° values are negative.

By FS the behavior of van't Hoff approach was linear, thus obtaining only a value for ΔH ° in the studied temperature rang. In addition, it was verified that the $\Delta H°_{FS}$ was higher than the $\Delta H°_{SPR}$. The $\Delta H°_{SPR}$ values are the sum of the energies absorbed and released at each interaction site. Thus, the values obtained by SPR suggest that the interactions that occur far from the Trp residues release more energy, contributing to lower values of $\Delta H°_{SPR}$ when compared to the $\Delta H°_{FS}$ value.

The same behavior was observed for TΔS°. At low temperatures, the TΔS° values were higher when compared to the higher temperatures. The TΔS° values are contributions of the configurational entropy change (ΔS_{conf}) due to the reduction of the degrees of freedom of the complex formed from the free molecules and the desolvation entropy change (ΔS_{des}), resulting from the release of water molecules from the layer of solvation of both molecules (bLF and CUR). Hence, $\Delta S° = \Delta S_{des} + \Delta S_{conf}$. The highest TΔS° values show that at low temperature, $|\Delta S_{des}| > |\Delta S_{conf}|$, providing a greater release of water molecules from the solvation shell of bLF and CUR when the complex is formed. At higher temperatures $|\Delta S_{conf}| > |\Delta S_{des}|$ then water molecules are less structured, and consequently the reduction of the degrees of freedom of the complex formed from the free molecules has a greater contribution than the release of the water molecules from the solvation layer.

The TΔS° values found by SPR (42.68 kJ mol^{-1}, 293.15 K) were lower than those found by fluorescence (91.50 kJ mol^{-1}, 293.15 K). Probably processes such as conformational changes and desolvation of the interaction sites identified by SPR are different from the processes that occur in the interaction sites identified by the FS.

However, despite the remarkable variation of ΔH° and TΔS° as function of the temperature, the ΔG° values showed a weak variation. This type of behavior suggest the occurrence of the well known enthalpy–entropy compensation (EEC) [44]. To confirm the occurrence of this phenomenon in our studies we plotted a plot of ΔH° vs TΔS° (Figure 4).

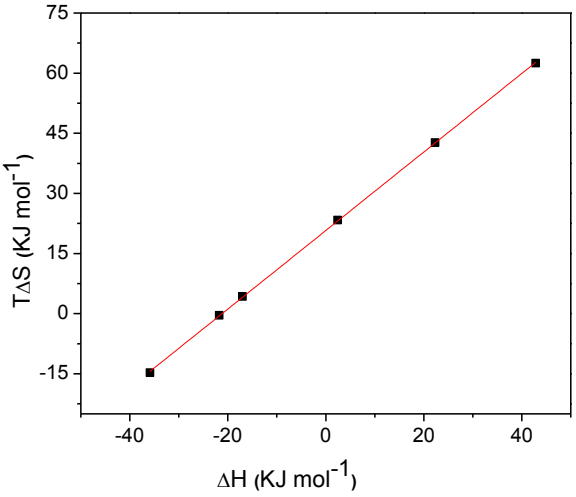

Figure 4: Enthalpy–entropy compensation plot of bLF-CUR binding.

The EEC phenomenon found in Figure 4 can be described by a increase in enthalpy offset by a increase in entropy. A linear relationship was obtained with slope and intercept (α and β) equal to 0.97 and 20.73, respectively. The slope near of unity suggests that ΔH° are often compensated by TΔS°[45], that is, ΔH° and TΔS° increase in the same proportion. The increment of entropy may be attributed the release of water from solvation layer of interacting molecules. However, this increase of entropy is compensated by the energy absorption for the break of H_2O-H_2O interaction.

Through the dependence of ΔH° with the temperature, it was possible to determine the standard heat capacity change, ΔCp°, using the relation: $\Delta C_p^o = \left(\frac{\partial H^\circ}{\partial T}\right)_P$ (Figure 5) (Table 3).

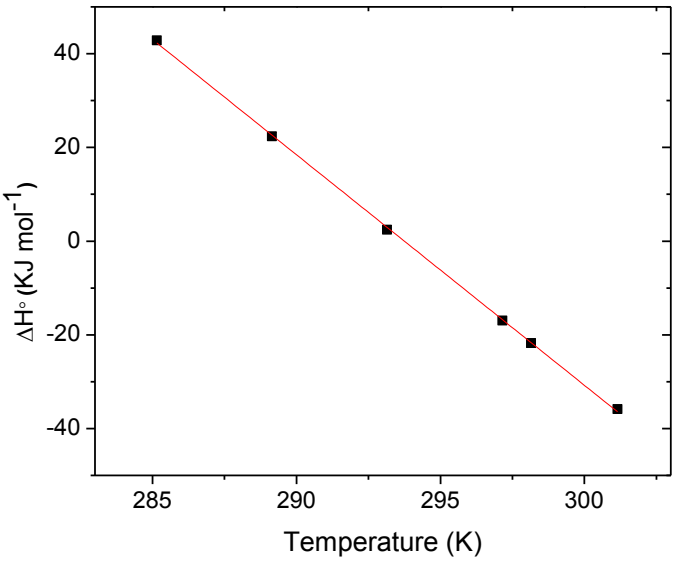

Figure 5: Plot of variation of the standard molar enthalpy change (ΔH°) *versus* temperature for the bLF-CUR binding.

The heat capacity change values provide information about energy and structural modifications from the interaction. Considering that $\Delta C_p^o = C_{p-bLF-CURC}^o - (C_{p-bLF}^o + C_{p-CURC}^o)$, a negative ΔC_p^o indicates that the bLF-CUR complex has less ability to transfer heat energy from the surroundings to the molecular potential energy component than the free bLF and CUR molecules. During complex formation (bLF-CUR) some intramolecular interaction of free molecules are broken while some new intermolecular interactions are formed. Furthermore, it is known that the desolvation of water molecules from the surface of the protein and CUR results in negative values of ΔCp° [46,47] . This can be confirmed by the analysis of Tds values, which shows a contribution of the increase in the degree of freedom of the system due to the release of water molecules from the solvation layer.

3.2.1. Energetic parameters of formation of bLF-CUR activated complex

The dependence of k_a and k_d on the temperature change yields the determination of the kinetic energetic parameters related to the formation of an activated bLF-CUR complex, formed from the association of free bLF and CUR

molecules or from the dissociation of the thermodynamic stable bLF-CUR complex [48,49]. These kinetic parameters are important because they provide information on potential energy and molecular dynamics changes associated with the activated complex formation.

Applying the Arrhenius approach of k_a and k_d on temperature (Figure S2), the activation energy for association of free bLF and CUR molecules ($E_{act(a)}$) and for dissociation of bLF-CUR thermodynamic stable complex ($E_{act(d)}$) to activated complex formation were obtained.

$$E_{act(x)} = -R\frac{\partial lnk_x}{\partial \frac{1}{T}} \quad (10)$$

In this equation, $E_{act(x)}$ is the activation energy for association or dissociation, *R* is the universal gas constant (8.3145 J·mol^{-1}·K^{-1}), k_x is the kinetic rate constant of association (M^{-1}s^{-1}) or dissociation (s^{-1}) and *T* is the temperature (K).

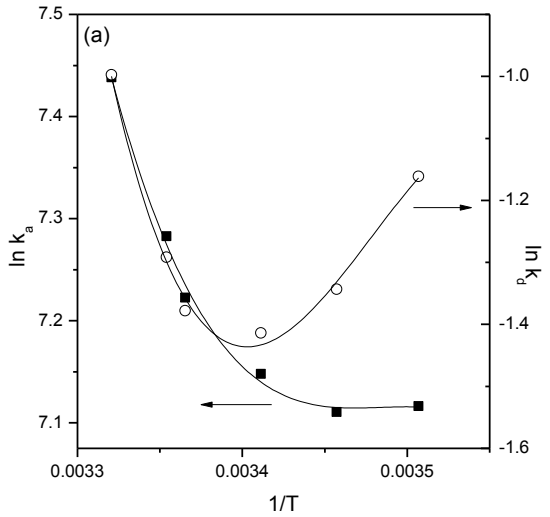

Figure S2 - ln k_a (■) and ln k_d (○) versus the inverse of temperatures associated with the interaction between bovine lactoferrin and curcumin at a pH of 7.4. Polynomial equation for association process: $lnk_a = 1.62 \times 10^7 \left(1/_T\right)^2 - 1.12 \times 10^6 \left(1/_T\right) + 201.58$; $R^2 = 0.97$, and for dissociation process: $lnk_d = 4.06 \times 10^7 \left(1/_T\right)^2 - 2.78 \times 10^6 \left(1/_T\right) + 437.17$; $R^2 = 0.89$.

The kinetic enthalpy change ($\Delta H_x^{\ddagger}$), the Gibbs free energy change ($\Delta G_x^{\ddagger}$) and the entropic terms ($T\Delta S_x^{\ddagger}$) of association and dissociation phases to activated complex formation were calculated using the equations 11 to 13.

$$\Delta H_x^{\ddagger} = E_{act(x)} - RT \tag{11}$$

$$\Delta G_x^{\ddagger}(T) = -RTln(k_x h/K_{B)} \tag{12}$$

$$T\Delta S_x^{\ddagger} = \Delta H_x^{\ddagger} - \Delta G_x^{\ddagger} \tag{13}$$

Here, *R* is the universal gas constant (8.3145 J·mol^{-1}·K^{-1}), *T* is the temperature (K), h is the Planck constant (6.626 × 10^{-34} J.s) and K_B is the Boltzmann's constant (1.38 × 10^{-23} J.K^{-1}).

The values of the kinetic parameters for the association and the dissociation phases are shown in Figure 6 (a) and (b), respectively.

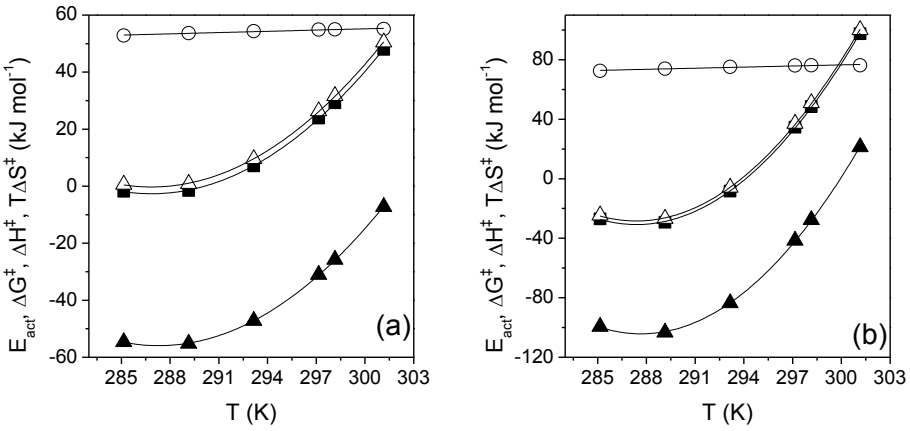

Figure 6 – Plot of kinetic activation energetic parameters *versus* temperature: (Δ) E_{act}, (○) $\Delta G^{\ddagger}$, (■) $\Delta H^{\ddagger}$, and (▲) $T\Delta S^{\ddagger}$ for (a) association and (b) dissociation phases.

The $E_{act(a)}$, $\Delta H_a^{\ddagger}$, and $T\Delta S_a^{\ddagger}$ values showed an increasing second-order polynomial behavior as a function of temperature (Fig. 6), revealing that above 290 K these energetic parameters increased.

The formation of bLF-CUR activated complex is dependent on the following processes: i) bLF and CUR desolvation, ii) change in the bLF binding site conformation, and iii) bLF-CUR interaction, being only the last resulting in energy releasing. Therefore, it is reasonable to propose that at low temperatures CUR interacted at bLF interface; while small degree of desolvation and conformational site change however, with the increase in the temperature, the bioactive molecule penetrates into the inner of the protein, and thus there is desolvation of CUR and bLF-binding site and also change this binding site conformation, resulting in the increasing of $E_{act(a)}$, $\Delta H_a^{\ddagger}$, and $T\Delta S_a^{\ddagger}$ values, s shown in the hypothetical figure below (Figure 7).

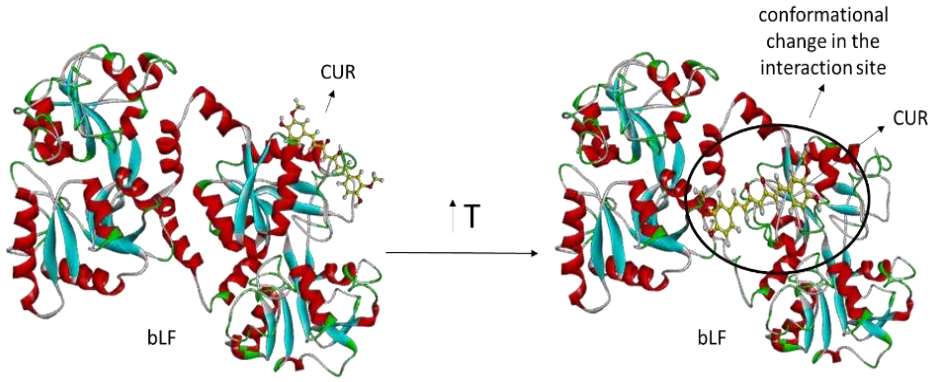

Figure 7 - The formation of bLF-CUR activated complex dependent on the temperature.

Interestingly, the coefficients of polynomial fitting for $\Delta H^{\ddagger}$, and $T\Delta S^{\ddagger}$ *vs.* T were very similar between themselves, for association (Eqs. 14 and 15) and dissociation phase (Eqs. 16 and 17). In addition, the $\Delta G_a^{\ddagger}$ and $\Delta G_d^{\ddagger}$ values maintained almost constant in this temperature range (Eqs. 18 and 19), indicating the occurrence "iso-kinetic comprensation" discussed above.

$$\Delta H_a^{\ddagger} = 0.24\,T^2 - 142.57\,T + 20446.23\,, R^2 = 0.99 \quad (14)$$

$$T\Delta S_a^{\ddagger} = 0.25\,T^2 - 145.91\,T + 20903.74, R^2 = 0.99 \quad (15)$$

$$\Delta H_d^{\ddagger} = 0.67\,T^2 - 390.53\,T + 56085.93\,, R^2 = 0.99 \quad (16)$$

$$T\Delta S_a^{\ddagger} = 0.69\,T^2 - 398.88\,T + 57270.41, R^2 = 0.99 \quad (17)$$

$$\Delta G_a^{\ddagger} = 0.14\,T + 11.08\,, R^2 = 0.96 \quad (18)$$

$$\Delta G_d^{\ddagger} = 0.24\,T + 2.19\,, R^2 = 0.92 \quad (19)$$

To confirm the occurrence "iso-kinetic comprensation phenomena in the association and dissociation phases to bLF-CUR activated complex formation, the $T\Delta S^{\ddagger}$ vs. $\Delta H^{\ddagger}$ data were plotted (Figure 8).

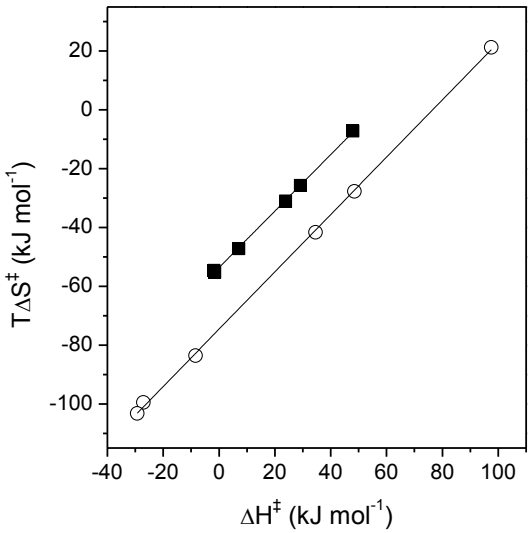

Figure 8 – $T\Delta S^{\ddagger}$ vs. $\Delta H^{\ddagger}$ plot for formation of bLF-CUR activated complex from: (■) association of free bLF and CUR (R^2 = 0.99), and (○) dissociation of thermodynamically stable bLF-CUR complex (R^2 = 0.99).

The slopes of each fitting were 0.9603 (R^2= 0.9993) and 0.9749 (R^2= 0.9995), for association and dissociation phases, respectively. In the context of formation of activated bLF-CUR complex, the EEC is mainly related to the desolvation phenomenon and to the change of conformation of the bLF-binding site, which cause an increase in the system enthalpy and in the entropy of the system.

4. Conclusions

The experimental results of this study provided thermodynamic and kinetic information on the interactions between bLF and CUR. Fluorescence data showed that fluorescence quenching of bLF was due to the formation of complexes with CUR, with one molecule of CUR bound to each bLF site. The thermodynamic parameters revealed that hydrophobic interactions were predominant in the bLF-CUR complex formation.

By SPR, we confirm the occurrence of interaction between CUR and bLF, and verify that the process of association of bLF and CUR molecules and dissociation of bLF-CUR complexes involves conformational changes in the protein. In addition, we have verified that the process of formation of the bLF-CUR complex is governed by a process known as enthalpy-entropy compensation. The kinetic study of the formation of bLF-CUR complex, suggests that at low temperatures the CUR interacts at the bLF interface, and with increasing temperature the CUR penetrates inside the protein.

The thermodynamic and kinetic parameters determined in this study are meaningful for a better understanding of the bLF-CUR binding process, further helpful in using this biofunctional complex in food formulations.

Acknowledgments

We are grateful to the Coordenação de Aperfeiçoamento de Pessoal de Nivel Superior – Brasil (CAPES) – Finance Code 001, Conselho Nacional de Desenvolvimento Científico e Tecnológico (CNPq) and Fundação de Amparo à Pesquisa do Estado de Minas Gerais (FAPEMIG).

5. References

(1) Farnaud, S.; Evans, R. W. Lactoferrin - A multifunctional protein with antimicrobial properties. *Mol. Immunol.* **2003**, *40* (7), 395–405.

(2) Steijns, J. M.; van Hooijdonk, A. C. M. Occurrence, structure, biochemical properties and technological characteristics of lactoferrin. *Br. J. Nutr.* **2000**, *84* (S1).

(3) Croguennec, T.; Li, N.; Phelebon, L.; Garnier-Lambrouin, F.; Gésan-Guiziou, G. Interaction between lactoferrin and casein micelles in skimmed milk. *Int. Dairy J.* **2012**, *27* (1–2), 34–39.

(4) Darwish, S.; Mozaffari, S.; Parang, K.; Tiwari, R. Cyclic peptide conjugate of curcumin and doxorubicin as an anticancer agent. *Tetrahedron Lett.* **2017**, *58* (49), 4617–4622.

(5) Hussain, Z.; Thu, H. E.; Amjad, M. W.; Hussain, F.; Ahmed, T. A.; Khan, S. Exploring recent developments to improve antioxidant, anti-inflammatory and antimicrobial efficacy of curcumin: A review of new trends and future perspectives. *Mater. Sci. Eng. C* **2017**, *77*, 1316–1326.

(6) Ward, P. P.; Paz, E.; Conneely, O. M. Multifunctional roles of lactoferrin: A critical overview. *Cell. Mol. Life Sci.* **2005**, *62* (22), 2540–2548.

(7) Sreedhara, A.; Flengsrud, R.; Langsrud, T.; Kaul, P.; Prakash, V.; Vegarud, G. E. Structural characteristic, pH and thermal stabilities of apo and holo forms of caprine and bovine lactoferrins. *BioMetals* **2010**, *23* (6), 1159–1170.

(8) Ripolles, D.; Harouna, S.; Parrón, J. A.; Calvo, M.; Pérez, M. D.; Carramiñana, J. J.; Sánchez, L. Antibacterial activity of bovine milk lactoferrin and its hydrolysates prepared with pepsin, chymosin and microbial rennet against foodborne pathogen Listeria monocytogenes. *Int. Dairy J.* **2015**, *45*, 15–22.

(9) Iglesias-Figueroa, B. F.; Espinoza-Sánchez, E. A.; Siqueiros-Cendón, T. S.; Rascón-Cruz, Q. Lactoferrin as a nutraceutical protein from milk, an overview. *Int. Dairy J.* **2019**, *89*, 37–41.

(10) Bokkhim, H.; Bansal, N.; Grøndahl, L.; Bhandari, B. Interactions between different forms of bovine lactoferrin and sodium alginate affect the properties of their mixtures. *Food Hydrocoll.* **2015**, *48*, 38–46.

(11) Wakabayashi, H.; Yamauchi, K.; Takase, M. Lactoferrin research, technology

509 and applications. *Int. Dairy J.* **2006**, *16* (11), 1241–1251.
510 (12) TOMITA, M.; WAKABAYASHI, H.; SHIN, K.; YAMAUCHI, K.; YAESHIMA, T.;
511 IWATSUKI, K. Twenty-five years of research on bovine lactoferrin applications.
512 *Biochimie* **2009**, *91* (1), 52–57.
513 (13) Yang, W.; Liu, F.; Xu, C.; Yuan, F.; Gao, Y. Molecular interaction between (-)-
514 epigallocatechin-3-gallate and bovine lactoferrin using multi-spectroscopic
515 method and isothermal titration calorimetry. *Food Res. Int.* **2014**, *64*, 141–149.
516 (14) Ferraro, V.; Madureira, A. R.; Sarmento, B.; Gomes, A.; Pintado, M. E. Study of
517 the interactions between rosmarinic acid and bovine milk whey protein α-
518 Lactalbumin, β-Lactoglobulin and Lactoferrin. *Food Res. Int.* **2015**, *77*, 450–459.
519 (15) Jain, B. A spectroscopic study on stability of curcumin as a function of pH in
520 silica nanoformulations, liposome and serum protein. *J. Mol. Struct.* **2017**, *1130*,
521 194–198.
522 (16) Stankovic, I. Curcumin. *Joint FAO/WHO Expert Committee on Food Additives*.
523 2004, pp 1–8.
524 (17) Bharal, N.; Sahaya, K.; Jain, S.; Mediratta, P. K.; Sharma, K. K. Curcumin has
525 anticonvulsant activity on increasing current electroshock seizures in mice.
526 *Phyther. Res.* **2008**, *22* (12), 1660–1664.
527 (18) Noratto, G. D.; Jutooru, I.; Safe, S.; Angel-Morales, G.; Mertens-Talcott, S. U.
528 The drug resistance suppression induced by curcuminoids in colon cancer SW-
529 480 cells is mediated by reactive oxygen species-induced disruption of the
530 microRNA-27a-ZBTB10-Sp axis. *Mol. Nutr. Food Res.* **2013**, *57* (9), 1638–1648.
531 (19) Ying, M.; Huang, F.; Ye, H.; Xu, H.; Shen, L.; Huan, T.; Huang, S.; Xie, J.; Tian,
532 S.; Hu, Z.; et al. Study on interaction between curcumin and pepsin by
533 spectroscopic and docking methods. *Int. J. Biol. Macromol.* **2015**, *79*, 201–208.
534 (20) Shin, G. H.; Li, J.; Cho, J. H.; Kim, J. T.; Park, H. J. Enhancement of Curcumin
535 Solubility by Phase Change from Crystalline to Amorphous in Cur-TPGS
536 Nanosuspension. *J. Food Sci.* **2016**, *81* (2), N494–N501.
537 (21) Maiti, K.; Mukherjee, K.; Gantait, A.; Saha, B. P.; Mukherjee, P. K. Curcumin–

phospholipid complex: Preparation, therapeutic evaluation and pharmacokinetic study in rats. *Int. J. Pharm.* **2007**, *330* (1–2), 155–163.

(22) Wang, X.; Jiang, Y.; Wang, Y.-W.; Huang, M.-T.; Ho, C.-T.; Huang, Q. Enhancing anti-inflammation activity of curcumin through O/W nanoemulsions. *Food Chem.* **2008**, *108* (2), 419–424.

(23) Ge, Y.-S.; Jin, C.; Song, Z.; Zhang, J.-Q.; Jiang, F.-L.; Liu, Y. Multi-spectroscopic analysis and molecular modeling on the interaction of curcumin and its derivatives with human serum albumin: A comparative study. *Spectrochim. Acta Part A Mol. Biomol. Spectrosc.* **2014**, *124*, 265–276.

(24) Mangolim, C. S.; Moriwaki, C.; Nogueira, A. C.; Sato, F.; Baesso, M. L.; Neto, A. M.; Matioli, G. Curcumin–β-cyclodextrin inclusion complex: Stability, solubility, characterisation by FT-IR, FT-Raman, X-ray diffraction and photoacoustic spectroscopy, and food application. *Food Chem.* **2014**, *153*, 361–370.

(25) Esmaili, M.; Ghaffari, S. M.; Moosavi-Movahedi, Z.; Atri, M. S.; Sharifizadeh, A.; Farhadi, M.; Yousefi, R.; Chobert, J.-M.; Haertlé, T.; Moosavi-Movahedi, A. A. Beta casein-micelle as a nano vehicle for solubility enhancement of curcumin; food industry application. *LWT - Food Sci. Technol.* **2011**, *44* (10), 2166–2172.

(26) Hudson, E. A.; de Paula, H. M. C.; Ferreira, G. M. D.; Ferreira, G. M. D.; Hespanhol, M. do C.; da Silva, L. H. M.; Pires, A. C. dos S. Thermodynamic and kinetic analyses of curcumin and bovine serum albumin binding. *Food Chem.* **2018**, *242*, 505–512.

(27) García-Montoya, I. A.; Cendón, T. S.; Arévalo-Gallegos, S.; Rascón-Cruz, Q. Lactoferrin a multiple bioactive protein: An overview. *Biochim. Biophys. Acta - Gen. Subj.* **2012**, *1820* (3), 226–236.

(28) Sharma, S.; Sinha, M.; Kaushik, S.; Kaur, P.; Singh, T. P. C-lobe of lactoferrin: The whole story of the half-molecule. *Biochem. Res. Int.* **2013**, No. May.

(29) Bollimpelli, V. S.; Kumar, P.; Kumari, S.; Kondapi, A. K. Neuroprotective effect of curcumin-loaded lactoferrin nano particles against rotenone induced neurotoxicity. *Neurochem. Int.* **2016**, *95*, 37–45.

(30) Atrahimovich, D.; Vaya, J.; Tavori, H.; Khatib, S. Glabridin Protects Paraoxonase 1 from Linoleic Acid Hydroperoxide Inhibition via Specific Interaction: A Fluorescence-Quenching Study. *J. Agric. Food Chem.* **2012**, *60* (14), 3679–3685.

(31) Schasfoort, R. B. M.; Tudos, A. J. *Handbook of Surface Plasmon Resonance*; 2013; Vol. 53.

(32) Atale, S. S.; Dyawanapelly, S.; Jagtap, D. D.; Jain, R.; Dandekar, P. Understanding the nano-bio interactions using real-time surface plasmon resonance tool. *Int. J. Biol. Macromol.* **2019**, *123*, 97–107.

(33) Gombau, J.; Nadal, P.; Canela, N.; Gómez-Alonso, S.; García-Romero, E.; Smith, P.; Hermosín-Gutiérrez, I.; Canals, J. M.; Zamora, F. Measurement of the interaction between mucin and oenological tannins by Surface Plasmon Resonance (SPR); relationship with astringency. *Food Chem.* **2019**, *275*, 397–406.

(34) de Paula, H. M. C.; Coelho, Y. L.; Agudelo, A. J. P.; Rezende, J. de P.; Ferreira, G. M. D.; Ferreira, G. M. D.; Pires, A. C. dos S.; da Silva, L. H. M. Kinetics and thermodynamics of bovine serum albumin interactions with Congo red dye. *Colloids Surfaces B Biointerfaces* **2017**, *159*, 737–742.

(35) Bi, H.; Tang, L.; Gao, X.; Jia, J.; Lv, H. Spectroscopic analysis on the binding interaction between tetracycline hydrochloride and bovine proteins β-casein, α-lactalbumin. *J. Lumin.* **2016**, *178*, 72–83.

(36) Lakowicz, J. R. *Principles of fluorescence spectroscopy*; 2006.

(37) Silva, M. S.; García-Estévez, I.; Brandão, E.; Mateus, N.; de Freitas, V.; Soares, S. Molecular Interaction Between Salivary Proteins and Food Tannins. *J. Agric. Food Chem.* **2017**, *65* (31), 6415–6424.

(38) Lelis, C. A.; Hudson, E. A.; Ferreira, G. M. D.; Ferreira, G. M. D.; da Silva, L. H. M.; da Silva, M. do C. H.; Pinto, M. S.; Pires, A. C. dos S. Binding thermodynamics of synthetic dye Allura Red with bovine serum albumin. *Food Chem.* **2017**, *217*, 52–58.

(39) Nunes, N. M.; Pacheco, A. F. C.; Agudelo, Á. J. P.; da Silva, L. H. M.; Pinto, M. S.; Hespanhol, M. do C.; Pires, A. C. dos S. Interaction of cinnamic acid and methyl cinnamate with bovine serum albumin: A thermodynamic approach. *Food Chem.* **2017**, *237*, 525–531.

(40) Mohammadi, F.; Moeeni, M. Study on the interactions of trans-resveratrol and curcumin with bovine α-lactalbumin by spectroscopic analysis and molecular docking. *Mater. Sci. Eng. C* **2015**, *50*, 358–366.

(41) Mohammadi, F.; Bordbar, A.-K.; Divsalar, A.; Mohammadi, K.; Saboury, A. A. Interaction of Curcumin and Diacetylcurcumin with the Lipocalin Member β-Lactoglobulin. *Protein J.* **2009**, *28* (3–4), 117–123.

(42) Bolel, P.; Mahapatra, N.; Halder, M. Optical Spectroscopic Exploration of Binding of Cochineal Red A with Two Homologous Serum Albumins. *J. Agric. Food Chem.* **2012**, *60*, 3727–3734.

(43) Patching, S. G. Surface plasmon resonance spectroscopy for characterisation of membrane protein–ligand interactions and its potential for drug discovery. *Biochim. Biophys. Acta - Biomembr.* **2014**, *1838* (1), 43–55.

(44) Ferrante, A.; Gorski, J. Enthalpy-entropy compensation and cooperativity as thermodynamic epiphenomena of structural flexibility in ligand-receptor interactions. *J. Mol. Biol.* **2012**, *417* (5), 454–467.

(45) Bou-Abdallah, F.; Sprague, S. E.; Smith, B. M.; Giffune, T. R. Binding thermodynamics of Diclofenac and Naproxen with human and bovine serum albumins: A calorimetric and spectroscopic study. *J. Chem. Thermodyn.* **2016**, *103*, 299–309.

(46) Niedzwiecka, A.; Stepinski, J.; Darzynkiewicz, E.; Sonenberg, N.; Stolarski, R. Positive Heat Capacity Change upon Specific Binding of Translation Initiation Factor eIF4E to mRNA 5 ‘ Cap Positive Heat Capacity Change upon Specific Binding of Translation Initiation Factor eIF4E to mRNA 5 ′ Cap †. *Biochemistry* **2002**, 12140–12148.

(47) Perozzo, R.; Folkers, G.; Scapozza, L. Thermodynamics of protein-ligand

interactions: History, presence, and future aspects. *J. Recept. Signal Transduct.* **2004**, *24* (1–2), 1–52.

(48) Smith, I. W. M. The temperature-dependence of elementary reaction rates: beyond Arrhenius. *Chem. Soc. Rev.* **2008**, *37* (4), 812–826.

(49) Pan, A.; Biswas, T.; Rakshit, A. K.; Moulik, S. P. Enthalpy–Entropy Compensation (EEC) Effect: A Revisit. *J. Phys. Chem. B* **2015**, *119* (52), 15876–15884.

(50) Cheng, L.-Y.; Xia, W.; Zhang, X.; Bai, A.-M.; Ouyang, Y.; Hu, Y.-J. In vitro binding comparison of cephalosporins to human serum albumin by spectroscopy and molecular docking approaches: A novel structural pursuing. *J. Mol. Liq.* **2017**, *248*, 168–176.

(51) KuKanich, B.; Gehring, R.; Webb, A. I.; Craigmill, A. L.; Riviere, J. E. Effect of formulation and route of administration on tissue residues and withdrawal times. *J. Am. Vet. Med. Assoc.* **2005**, *227* (10), 1574–1577.

(52) Martins, M. T.; Barreto, F.; Hoff, R. B.; Jank, L.; Arsand, J. B.; Motta, T. M. C.; Schapoval, E. E. S. Multiclass and multi-residue determination of antibiotics in bovine milk by liquid chromatography–tandem mass spectrometry: Combining efficiency of milk control and simplicity of routine analysis. *Int. Dairy J.* **2016**, *59*, 44–51.

(53) BROWN, S. A. Fluoroquinolones in animal health. *J. Vet. Pharmacol. Ther.* **1996**, *19* (1), 1–14.

(54) Attili, A. R.; Preziuso, S.; Ngu Ngwa, V.; Cantalamessa, A.; Moriconi, M.; Cuteri, V. Clinical evaluation of the use of enrofloxacin against Staphylococcus aureus clinical mastitis in sheep. *Small Rumin. Res.* **2016**, *136*, 72–77.

(55) Giguère, S.; Dowling, P. M. Fluoroquinolones. In *Antimicrobial Therapy in Veterinary Medicine*; John Wiley & Sons, Inc: Hoboken, NJ, 2013; pp 295–314.

(56) Idowu, O. R.; Peggins, J. O.; Cullison, R.; Bredow, J. von. Comparative pharmacokinetics of enrofloxacin and ciprofloxacin in lactating dairy cows and beef steers following intravenous administration of enrofloxacin. *Res. Vet. Sci.*

654 **2010**, *89* (2), 230–235.
655 (57) Liu, Z.; Chan, L.; Ye, X.; Bai, Y.; Chen, T. BSA-Based Cu 2 Se Nanoparticles
656 with Multistimuli-Responsive Drug Vehicles for Synergistic Chemo-Photothermal
657 Therapy. *Colloids Surfaces B Biointerfaces* **2018**.
658 (58) Salehiabar, M.; Nosrati, H.; Javani, E.; Aliakbarzadeh, F.; Kheiri Manjili, H.;
659 Davaran, S.; Danafar, H. Production of biological nanoparticles from bovine
660 serum albumin as controlled release carrier for curcumin delivery. *Int. J. Biol.*
661 *Macromol.* **2018**, *115*, 83–89.
662 (59) McCann, D.; Barrett, A.; Cooper, A.; Crumpler, D.; Dalen, L.; Grimshaw, K.;
663 Kitchin, E.; Lok, K.; Porteous, L.; Prince, E.; et al. Food additives and
664 hyperactive behaviour in 3-year-old and 8/9-year-old children in the community:
665 a randomised, double-blinded, placebo-controlled trial. *Lancet* **2007**, *370* (9598),
666 1560–1567.
667 (60) Lin, Y.; Jiao, G.; Sun, G.; Zhang, L.; Wang, S.; Liu, H.; Li, Z. Binding of
668 teicoplanin and vancomycin to bovine serum albumin in vitro: A
669 multispectroscopic approach and molecular modeling. *Luminescence* **2014**, *29*
670 (2), 109–117.
671 (61) Jattinagoudar, L.; Meti, M.; Nandibewoor, S.; Chimatadar, S. Evaluation of the
672 binding interaction between bovine serum albumin and dimethyl fumarate, an
673 anti-inflammatory drug by multispectroscopic methods. *Spectrochim. Acta - Part*
674 *A Mol. Biomol. Spectrosc.* **2016**, *156*, 164–171.
675 (62) Guo, M.; Lu, W.-J.; Yi, P.-G.; Yu, Q.-S. Study on the thermodynamic
676 characteristics between fluoroquinolone and bovine serum albumin. *J. Chem.*
677 *Thermodyn.* **2007**, *39* (3), 337–343.
678 (63) Seedher, N.; Agarwal, P. Complexation of fluoroquinolone antibiotics with human
679 serum albumin: A fluorescence quenching study. *J. Lumin.* **2010**, *130* (10),
680 1841–1848.
681 (64) Liu, B.; Xue, C.; Wang, J.; Yang, C.; Lv, Y. Study of the quenching mechanism
682 of bovine serum albumin with presence of chloramphenicol and enrofloxacin.

683 *Phys. Chem.* **2011**, *6* (2).
684 (65) Ni, Y.; Su, S.; Kokot, S. Spectrometric studies on the interaction of
685 fluoroquinolones and bovine serum albumin. *Spectrochim. Acta - Part A Mol.*
686 *Biomol. Spectrosc.* **2010**, *75* (2), 547–552.
687 (66) Reddy, T. K.; Srikanth, G.; Mallikarjun, V.; Nivethithai, P. MECHANISM OF
688 INTERACTION OF SOME ANTIMICROBIAL AGENTS WITH BOVINE SERUM
689 ALBUMIN. *J. Glob. Pharma Technol.* **2009**, *2* (March 2010), 47–55.
690 (67) Qin, P.; Pan, X.; Liu, R.; Hu, C.; Dong, Y. Toxic interaction mechanism of two
691 fluoroquinolones with serum albumin by spectroscopic and computational
692 methods. *J. Environ. Sci. Heal. - Part B Pestic. Food Contam. Agric. Wastes*
693 **2017**, *52* (11), 833–841.
694 (68) Wang, L.; Zhang, G.; Wang, Y. Binding properties of food colorant allura red with
695 human serum albumin in vitro. *Mol. Biol. Rep.* **2014**, *41* (5), 3381–3391.
696 (69) Ma, L.; Liu, B.; Wang, C.; Zhang, H.; Cheng, X. The Investigation of
697 Fluorescence Spectra and Fluorescence Quantum Yield of Enrofloxacin. **2018**, *2*
698 (1), 11–16.
699 (70) Lizondo, M.; Pons, M.; Gallardo, M.; Estelrich, J. Physicochemical properties of
700 enrofloxacin. *J. Pharm. Biomed. Anal.* **1997**, *15* (12), 1845–1849.
701 (71) Bi, S.; Song, D.; Tian, Y.; Zhou, X.; Liu, Z.; Zhang, H. Molecular spectroscopic
702 study on the interaction of tetracyclines with serum albumins. *Spectrochim. Acta*
703 *- Part A Mol. Biomol. Spectrosc.* **2005**, *61* (4), 629–636.
704 (72) Schneider, M. J. Rapid Fluorescence Screening Assay for Enrofloxacin and
705 Tetracyclines in Chicken Muscle. *J. Agric. Food Chem.* **2004**, *52* (26), 7809–
706 7813.
707 (73) Yazdi, S. R.; Corredig, M. Heating of milk alters the binding of curcumin to
708 casein micelles . A fluorescence spectroscopy study. *Food Chem.* **2012**, *132* (3),
709 1143–1149.
710 (74) Benesi, H. A.; Hildebrand, J. H. a Spectrophotometric Investigation of the
711 Interaction of Iodine With Aromatic Hydrocarbons. *J. Am. Chem. Soc.* **1949**, *71*

(8), 2703–2707.

(75) Bensouilah, N.; Abdaoui, M. Inclusion complex of N-nitroso, N-(2-chloroethyl), N`, N`-dibenzylsulfamid with β-Cyclodextrin: Fluorescence and molecular modeling. *Comptes Rendus Chim.* **2012**, *15* (11–12), 1022–1036.

(76) Otagiri, M. A Molecular Functional Study on the Interactions of Drugs with Plasma Proteins. *Drug Metab. Pharmacokinet.* **2005**, *20* (5), 309–323.

(77) Roy, S. Review on Interaction of Serum Albumin with Drug Molecules. *Res. Rev. J. Pharmacol. Toxicol. Stud.* **2016**, *4* (2), 1–10.

(78) Ming Guo, Wei-Jun Lu, Ping-Gui Yi, Q.-S. Y. Study on the thermodynamic characteristics between fluoroquinolone and bovine serum albumin. *J. Chem. Thermodyn.* **2007**, *39*, 337–343.

(79) Sinisi, V.; Forzato, C.; Cefarin, N.; Navarini, L.; Berti, F. Interaction of chlorogenic acids and quinides from coffee with human serum albumin. *FOOD Chem.* **2015**, *168*, 332–340.

(80) Bourassa, P.; Kanakis, C. D.; Tarantilis, P.; Pollissiou, M. G.; Tajmir-Riahi, H. a. Resveratrol, genistein, and curcumin bind bovine serum albumin. *J. Phys. Chem. B* **2010**, *114* (9), 3348–3354.

(81) Pal, U.; Pramanik, S. K.; Bhattacharya, B.; Banerji, B.; Maiti, N. C. Binding interaction of a novel fluorophore with serum albumins: steady state fluorescence perturbation and molecular modeling analysis. *Springerplus* **2015**, *4* (1).

(82) Li, M.; Hagerman, A. E. Role of the Flavan-3-ol and Galloyl Moieties in the Interaction of (−)-Epigallocatechin Gallate with Serum Albumin. *J. Agric. Food Chem.* **2014**, *62* (17), 3768–3775.

(83) Datta, S.; Mahapatra, N.; Halder, M. pH-insensitive electrostatic interaction of carmoisine with two serum proteins: A possible caution on its uses in food and pharmaceutical industry. *J. Photochem. Photobiol. B Biol.* **2013**, *124*, 50–62.

(84) Majorek, K. A.; Porebski, P. J.; Dayal, A.; Zimmerman, M. D.; Jablonska, K.; Stewart, A. J.; Chruszcz, M.; Minor, W. Structural and immunologic

741 characterization of bovine, horse, and rabbit serum albumins. *Mol. Immunol.*
742 **2012**, *52* (3–4), 174–182.
743 (85) Khatun, S.; Riyazuddeen; Yasmeen, S.; Kumar, A.; Subbarao, N. Calorimetric,
744 spectroscopic and molecular modelling insight into the interaction of gallic acid
745 with bovine serum albumin. *J. Chem. Thermodyn.* **2018**, *122*, 85–94.
746 (86) Kaur, A.; Khan, I. A.; Banipal, P. K.; Banipal, T. S. Deciphering the complexation
747 process of a fluoroquinolone antibiotic, levofloxacin, with bovine serum albumin
748 in the presence of additives. *Spectrochim. Acta - Part A Mol. Biomol. Spectrosc.*
749 **2018**, *191*, 259–270.
750 (87) Yuan, J.-L.; lv, Z.; Liu, Z.-G.; Hu, Z.; Zou, G.-L. Study on interaction between
751 apigenin and human serum albumin by spectroscopy and molecular modeling. *J.*
752 *Photochem. Photobiol. A Chem.* **2007**, *191* (2–3), 104–113.
753 (88) Ross, P. D.; Subramanian, S. Thermodynamics of protein association reactions:
754 forces contributing to stability. *Biochemistry* **1981**, *20* (11), 3096–3102.
755 (89) Cui, F.-L.; Wang, J.-L.; Cui, Y.-R.; Li, J.-P. Fluorescent investigation of the
756 interactions between N-(p-chlorophenyl)-N′-(1-naphthyl) thiourea and serum
757 albumin: Synchronous fluorescence determination of serum albumin. *Anal.*
758 *Chim. Acta* **2006**, *571* (2), 175–183.
759 (90) Basu, A.; Kumar, G. S. Thermodynamics of the interaction of the food additive
760 tartrazine with serum albumins: a microcalorimetric investigation. *Food Chem.*
761 **2015**, *175*, 137–142.
762 (91) Bou-Abdallah, F.; Sprague, S. E.; Smith, B. M.; Giffune, T. R. Binding
763 thermodynamics of Diclofenac and Naproxen with human and bovine serum
764 albumins: A calorimetric and spectroscopic study. *J. Chem. Thermodyn.* **2016**,
765 *103*, 299–309.
766 (92) Chaires, J. B. Calorimetry and Thermodynamics in Drug Design. *Annu. Rev.*
767 *Biophys.* **2008**, *37* (1), 135–151.
768 (93) Chodera, J. D.; Mobley, D. L. Entropy-enthalpy compensation: Role and
769 ramifications in biomolecular ligand recognition and design. *Annu Rev Biophys*

2014, *42*, 121–142.

(94) Sturtevant, J. M. Heat capacity and entropy changes in processes involving proteins. *Proc. Natl. Acad. Sci.* **1977**, *74* (6), 2236–2240.

(95) Perozzo, R.; Folkers, G.; Scapozza, L. Thermodynamics of protein-ligand interactions: history, presence, and future aspects. *J. Recept. Signal Transduct. Res.* **2004**, *24* (1–2), 1–52.

(96) Saini, R. D. Thermodynamics of protein-ligand interactions and their analysis. *J. Proteins Proteomics* **2017**, *8* (4), 205–217.

(97) Ford, D. M. Enthalpy−Entropy Compensation is Not a General Feature of Weak Association. *J. Am. Chem. Soc.* **2005**, *127* (46), 16167–16170.

(98) Ball, V.; Maechling, C. Isothermal microcalorimetry to investigate non specific interactions in biophysical chemistry. *Int. J. Mol. Sci.* **2009**, *10* (8), 3283–3315.

(99) Molina-Bolívar, J. A.; Ruiz, C. C.; Galisteo-González, F.; O'Donnell, M. M.; Parra, A. Energetics of albumin-disuccinylmaslinic acid binding determined by fluorescence spectroscopy. *Fluid Phase Equilib.* **2015**, *400*, 43–52.

(100) Banerjee, T.; Singh, S. K.; Kishore, N. Binding of Naproxen and Amitriptyline to Bovine Serum Albumin: Biophysical Aspects. *J. Phys. Chem. B* **2006**, *110* (47), 24147–24156.

(101) Xu, Y.; Oruganti, S. V.; Gopalan, V.; Foster, M. P. Thermodynamics of coupled folding in the interaction of archaeal RNase P proteins RPP21 and RPP29. *Biochemistry* **2012**, *51* (4), 926–935.

(102) Spolar, R.; Record, M. Coupling of local folding to site-specific binding of proteins to DNA. *Science (80-.).* **1994**, *263* (5148), 777–784.

(103) Banipal, T. S.; Kaur, N.; Banipal, P. K. Binding studies of caffeine and theophylline to bovine serum albumin: Calorimetric and spectroscopic approach. *J. Mol. Liq.* **2016**, *223*, 1048–1055.

(104) Vega, S.; Abian, O.; Velazquez-Campoy, A. On the link between conformational changes, ligand binding and heat capacity. *Biochim. Biophys. Acta - Gen. Subj.* **2016**, *1860* (5), 868–878.

Capítulo 2: Interactions of enrofloxacin with bovine serum albumin: A detailed thermodynamic study by fluorescence spectroscopy

Abstract

A more comprehensive study of the thermodynamic parameters of BSA-ENRO complex formation is described in this paper, using fluorescence spectroscopy. Our study suggested that ENRO binds to subdomain IIA (site I) of BSA, interacting with the hydrophobic side chains and positively charged regions. The fluorescence spectroscopy results showed negative values of standard enthalpy and entropy changes ($\Delta H°$ = -74.07 to -36.54 kJ·mol^{-1} and $T\Delta S°$ = -45.88 to -11.12 kJ·mol-1·K^{-1}), indicating that the process of forming the BSA-ENRO complex is exothermic. The Gibbs free energy change standard values were negative ($\Delta G°$ = -28.19 to -25.42 kJ·mol^{-1}), however, it showed a small variation as a function of temperature. This behavior may be due to the occurrence of the enthalpy-entropy compensation (EEC), which was confirmed by the linearity of the $T\Delta S$ ° and $\Delta G°$ vs ΔH ° graph. It was also obtained in the study the standard heat capacity change, $\Delta Cp°$, which presented a value of 1.24 kJ K^{-1} mol^{-1}, thus showing that the complex formed between BSA and ENRO has a greater ability to transfer energy to the potential form than the free molecules. Thus, in this study we obtained a more detailed study of the interaction between BSA and ENRO, which is of great importance for future application studies.

Keywords: enrofloxacin, bovine serum albumin, fluorescence spectroscopy

1. Introduction

The use of antibiotics in the treatment of bacterial infections has triggered global attention from the point of view of food safety[50–52]. The main features of antimicrobial

826 agent are its high bioavailability, low toxicity to the host, and excellent penetration into
827 the fabric[53,54]. However, drug residues can be found in food like milk when good
828 veterinary practices are not performed.

829 Enrofloxacin (ENRO) was the first synthetic fluoroquinolone introduced and
830 approved as an antibacterial agent developed for veterinary application, highly effective
831 against a broad spectrum of Gram-positive and Gram-negative bacteria[55]. It is
832 registered in several countries including the US and Europe, with potential for the
833 treatment of infections in cow[56].

834 The study on the effect/influence of drugs on the protein constituents of the
835 circulatory system is of great interest, since the interaction of the drugs with the
836 transport proteins can affect both the availability of the drug and the functioning of the
837 proteins. One of the functions of transport proteins is their effective role in the delivery
838 of drugs and other substances[57,58], thus playing an important in biological processes.

839 The serum albumins have been used for initial studies with drug. The binding
840 capacity of a drug with serum albumin is important to efficacy as an agent
841 pharmaceutical, since the serum albumins are the major proteins responsible for drug
842 delivery in their target organs.

843 Bovine serum albumin (BSA) is the major protein in cow blood plasma and
844 plays important physiological role in the transport of hydrophobic compounds[59]. Also, it
845 is present in milk, arranged in a helical protein conformation heart-shaped consisting of
846 three homologous sites (I, II, III), each domain consists of two separate sites[60,61]. Many
847 studies of interaction between proteins and drugs use BSA because of their low cost,
848 availability, binding ability and its identity homology (~76%) to human serum albumin
849 (HSA). Thus, BSA can be used as a model protein for the study of protein-drug
850 interaction, providing valuable information.

851 Despite the several reports in the literature on the interaction of ENRO with
852 transport proteins, BSA and HSA[62–67], a comprehensive understanding of the
853 thermodynamic parameters of formation of the BSA-ENRO complex should still be fully

understood. For this purpose, all thermodynamic parameters of interaction (ΔG°, ΔS°, ΔH° and ΔCp°) as well as their detailed contributions were analyzed in this work. In addition, all the studies reported so far on the interaction between BSA and ENRO are based on changes in protein properties, such as the reduction of their intrinsic fluorescence. In our study, ENRO's ability to emit fluorescence will be used to determine the thermodynamic parameters of the BSA-ENRO interaction.

Thus the work aims at a more detailed study of the interaction between BSA and ENRO using fluorescence spectroscopy.

2. Material and Methods

2.1. Material

BSA (>99% wt.), ENRO (>98% wt.), warfarin (analytical standard), ibuprofen (>98% wt.), digitoxin (>92% wt.) and sodium phosphate (reagent grade) were purchased from Sigma-Aldrich (St. Louis, MO, USA).

2.2. Fluorescence experiments

2.2.1. BSA-ENRO binding

Fluorescence spectra were obtained with a LS55 Fluorescence (Perkin Elmer) spectrofluorimeter equipped with a thermostat bath, according to the procedure of Wang et al. with some modifications[68]. Initially a solution of ENRO 1.0×10^{-3} mol·L^{-1} in DMSO was prepared. From this solution was prepared the stock solution of ENRO 1.5×10^{-5} mol·L^{-1}, in solution of BSA 3.0×10^{-7} mol·L^{-1}. For fluorescence measurements, 10 titrations of 40 µL of a stock solution of ENRO (3×10^{-7} mol·L^{-1} to 3×10^{-6} mol·L^{-1}) in 2.0 mL of BSA solution (3.0×10^{-7} mol·L^{-1}) in a quartz cell and at pH 7.4 were used. To minimize the effect of 10 titrations of ENRO containing DMSO on the protein, we added 1.5% DMSO to the BSA solution in a quartz cell. Fluorescence emission spectra were then measured at five different temperatures (293.15, 298.15, 308.15 and 323.15 K) in the range 315–600 nm (excitation wavelength, 315 nm).

2.2.2. Competitive binding studies

The competitive binding studies were carried out using site probes for sites I, II and III of BSA (warfarin, ibuprofen and digitoxin, respectively). For this, BSA and site probes were at fixed concentration (3.00 x 10^{-7} mol.L^{-1}) and the fluorescence quenching titration (with ENRO) was performer as described before at pH 7.4. Thus, binding parameters for ENRO-BSA binding were determined in the presence of site markers.

3. Results and Discussion

3.1. Binding of ENRO on BSA studied by fluorescence spectroscopy

The ENRO molecule contains in its structure a carboxyl group and a piperazinyl amine group whose fluorescence emission is related to the degree of protonation and is therefore pH dependent [69]. ENRO can emit fluorescence at pH around 7.0 when excited at 275 and 315 nm [70]. However, the wavelength 275 nm is very close to the wavelength of excitation BSA [71], thus we choose to excite ENRO at 315 nm [72], wavelength in which the protein did not absorbs radiation (Figure 1 (A)).

The fluorescence emission spectra of ENRO showed a strong fluorescence emission peak at 415 nm, which enhanced with increasing ENRO concentration in the system (Figure 1 (A)).

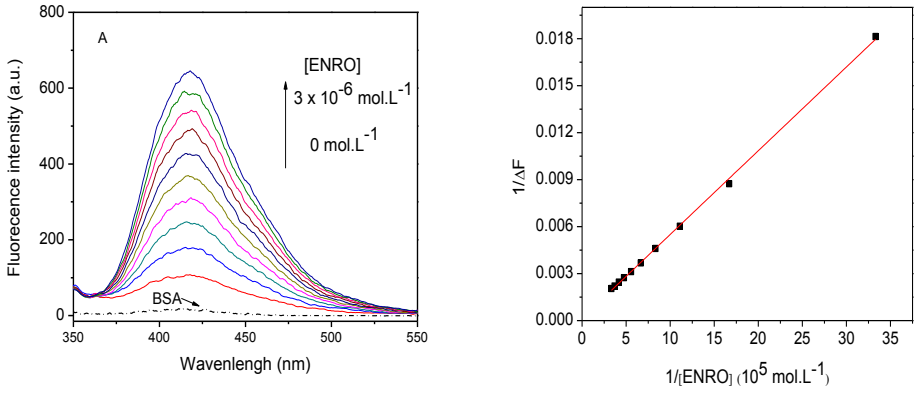

Figure 1: (A) - Fluorescence spectra of increasing ENRO concentration at 308.15 K and pH 7.4 (λ_{ex}= 315 nm and λ_{em}= 415 nm) in the presence of BSA (3.0 x 10^{-7} mol.L^{-1}). Arrow indicates an increase in the ENRO concentration (from 0 to 3.0 x 10^{-6} mol.L^{-1}). (B) - The double reciprocal plot was obtained on the basis of (1), allowing

calculation of the inclusion constant value of the complexes of ENRO and the studied BSA.

The relationship between the inverse of fluorescence emitted by ENRO *vs* the inverse of its concentration, through the Benesi-Hildebrand model (Equation 1), yields the binding constant (K_b) for the ENRO−BSA complex formation[73,74].

$$\frac{1}{\Delta F} = \frac{1}{\Delta F_{máx}} + \frac{1}{(K_b\, \Delta F_{máx}\, [ENRO])} \quad (1)$$

where ΔF is the difference in fluorescence intensity between the sample, with and without enrofloxacin, $\Delta F_{máx}$ is the value of maximum ΔF at plateau, K_b is the binding constant, and [ENRO] is the concentration of enrofloxacin (mol.L^{-1}).

A linearity (r = 0.99) of the curve in the plot 1/ΔF *vs.* 1/[ENRO] indicated that the complex formation stoichiometry was 1:1, (Figure 1 (B))[75], i.e., for each ENRO molecule there is one BSA molecule.

The affinity of albumin for a particular drug is important to guide the transport of the drug in blood circulation and its release to the target site[76,77]. The K_b values (Table 1) ranged from 1.06 x 10^5 to 1.29 x 10^4 L.mol^{-1} for the temperatures studied at pH 7.4. The K_b decreased with the temperature increase indicating that the complex is more stable at lower temperatures; and considering that $K_b = [BSA - ENRO]/[BSA][ENRO]$, more complexes were formed at lower than at higher temperatures. The values of the K_b found by Qin et al., 2017 were of the order of 10^3 L.mol^{-1}, about 10 times lower than the value found in our study. The authors also observed variation in Kb values with temperature. At 293 K the value of Kb was 9.0 x 10^3 L.mol^{-1}, while at 320 K the value of Kb was 5.7 x 10^3 L.mol^{-1}, this variation of kb is 5 times smaller than the variation found in our study. This difference in the variation of K_b values can be justified by the use of the fluorescence emission property of different molecules (BSA and ENRO). In our study was used the fluorescence emission capability of ENRO, already in the study of Qin et al., 2017 they used the fluorescence emission property of BSA when excited at 280nm [67]. The K_b values found in our study are in agreement with values found in other

interaction studies between BSA and ENRO, with K_b values in the order of 10^{-4} L.mol^{-1} [78, 66,64].

Table 1 – The binding constant (K_b), standard enthalpy change (ΔH°), standard Gibbs free energy change (ΔG°) and standard entropy change (TΔS°) associated to formation of ENRO-BSA complex at pH = 7.4.

Temperature (K)	K_b (10^4 M^{-1})	ΔG° (KJ.mol^{-1})	ΔH° (KJ.mol^{-1})	TΔS° (kJ.mol^{-1})
293.15	10.6 ± 0.06	-28.19	-74.07	-45.88
298.15	6.76 ± 0.35	-27.55	-67.29	-39.74
308.15	2.94 ± 0.16	-26.35	-54.39	-28.04
323.15	1.29 ± 0,08	-25.42	-36.54	-11.12

To identify the ENRO binding site on BSA, we performed competitive binding experiments with three specific site probes. The use of probes that bind to specific sites on protein allows a simple and rapid screening about the link of local drug by macromolecule. BSA is made up of three homologous sites that are linearly arranged, structurally distinct, and evolutionarily related domains (I–III) [79,80], and are involved in transport of different molecules, such as drugs. The binding between BSA and drugs and/or any competitive molecule, such as other medicines, may determine the pharmacological effect of the drug[81]. It is known that warfarin binding specifically on site I of BSA, while ibuprofen and digitoxin are markers for BSA sites II and III, respectively [82,83].

In the presence of warfarin the K_b value was reduced by 68.64% (2.12 ± 0.12 x 10^4 L.mol^{-1}) compared to ENRO-BSA without any marker (6.76 ±0.41 x 10^4 L.mol^{-1}), while in the presence of ibuprofen and digitoxin it had a pronounced increase (K_b = 1.80 ± 0.09 x 10^5 L.mol^{-1} and K_b = 8.87 ± 0.09 x 10^4 L.mol^{-1}, respectively) . These results indicate that ENRO competes with warfarin for the same binding site in BSA, the subdomain II A, located inside site I. BSA exhibits about 76% sequence homology

and identity of tertiary structures to human serum albumin (HSA), which causes both molecules to have homologous binding sites[84,85]. In a study by Seedher and Agarwal, (2010) they found that ENRO competes with phenylbutazone for the same binding site (site I) as HSA, corroborating with our finding that ENRO binds preferentially to site I. Kaur et al., (2018) studied the interaction between BSA and levofloxacin, a drug with a chemical structure similar to ENRO. In the study the researchers found by molecular docking that levofloxacin binds preferentially to the site I of the BSA. These authors have verified the occurrence of hydrogen bonds, hydrophobic interactions, and other types of interactions like π-cation, charge-charge, and salt bridge between amino acids present in site I of BSA and regions (piperidone carbonyl, carboxylate, piperazine ring) present in the structure of levofloxacin, also present in the structure of ENRO. Qin et al. (2017) had suggested that ENRO binds to subdomain III A (site II) of the BSA. The internal cavity of subdomain IIA (site I) of BSA is formed by hydrophobic side chains, while the entrance of the pocket is surrounded by positively charged residues [87]. ENRO has in its structure hydrophobic group with the benzene ring and ionizable groups (-COOH and -NH) which may interact with the hydrophobic side chains and the charged residues of subdomain IIA of the protein, respectively. In addition, in the work of Qin et al. (2017), they used different markers in relation to those used in our study, which may justify the difference found in relation to the main interaction site of BSA for the ENRO molecule.

3.2. Thermodynamic parameters for ENRO–BSA binding

During the formation of complexes between proteins and ligands four main non-covalent bindings may occur, such as hydrogen bonding, van der Waals forces, electrostatic, and hydrophobic bindings. The determination of the thermodynamic binding parameters can help to elucidate the main forces involved in the process of complex formation between BSA and ENRO[88,89].

To elucidate the main forces of binding between BSA and ENRO, thermodynamic parameters, such as standard Gibbs free energy change (ΔG°), standard enthalpy change (ΔH°), standard entropy change (ΔS°), and standard heat capacity change ($\Delta C_p°$) for complex formation were determined.

The ΔGº values were directly calculated from K_b values at each temperature (Equation 2), the ΔHº values were determined by the non-linear van't Hoff approach (Equations 3 and 4, Figure 2), and the entropic term (TΔSº) were obtained using the fundamental Gibbs equation (Equation 5). The results are shown in Table 1.

$$\Delta G^0 = -RTlnK_b \quad (2)$$

$$lnK = a + b\left(\frac{1}{T}\right) + c\left(\frac{1}{T}\right)^2 + d\left(\frac{1}{T}\right)^3 + \cdots + \ln \Phi \quad (3)$$

$$\Delta H^\circ = -R\left[b + 2C\left(\frac{1}{T}\right) + 3d\left(\frac{1}{T}\right)^2 + \cdots\right] \quad (4)$$

$$\mathrm{T}\Delta S° = \Delta \mathrm{H}° - \Delta G^o \quad (5)$$

where *R* is the universal gas constant (8.3145 J.mol^{-1}.K^{-1}), *T* is the temperature (in K), K_b is the binding constant (L.mol^{-1}).

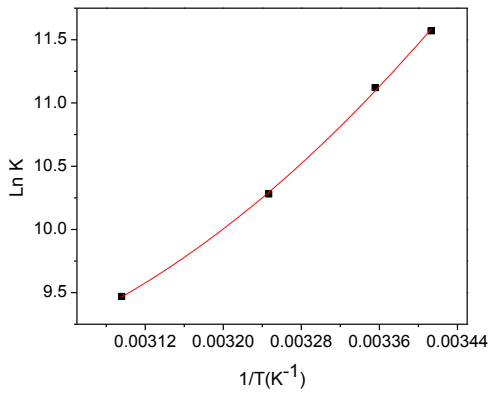

Figure 2: Non-linear van`t Hoff plot for binding of BSA (3.00 x 10^{-7} mol.L^{-1}) and ENRO at different temperatures (pH = 7.4).

The non-linear regression of the van`t Hoff plot (Figure 2) is common when the energy sources during the binding come from non-covalent binding[44].

As shown in Table 1 the ΔH° and TΔS° values were negative, being therefore the formation of the complex driven by the enthalpic term. Thus, the process of formation of the BSA-ENRO complex were exothermic.

The negative values of ΔH° found for the BSA-ENRO interaction are resultants of the contribution of three different processes demonstrated in the Equation 6.

$$\Delta H^0 = \Delta H_{des} + \Delta H_{mud.conf} + \Delta H_{BSA-ENRO} \quad (6)$$

Were, ΔH_{des} refers to desolvation of the bLF and CUR surfaces; $\Delta H_{mud.conf}$ is the conformational change of the bLF interaction site, and $\Delta H_{BSA-ENRO}$ is the formation of the BSA-ENRO interactions.

Considering that the values of ΔH ° were negative, it can be concluded that the contribution of the exothermic terms $\Delta H_{BSA-ENRO}$ was greater than the contribution of the endothermic terms ΔH_{des} and $\Delta H_{mud.conf}$.

In a similar way that was discussed for ΔH°, the entropic term (ΔS°) can be basically dismembered as shown in equation 7.

$$\Delta S° = \Delta S_{conf} + \Delta S_{solv} + \Delta S_{mud.conf} \quad (7)$$

Where, ΔS_{conf} is the configurational entropy change that reflects the reduction of degrees of freedom when the complex is formed from two free molecules in solution; ΔS_{solv} describes the entropy change resulting from the release of water molecules from the solvation shell of ENRO and BSA to form the BSA-ENRO complex; and $\Delta S_{mud.conf}$ refers to conformational changes in the protein interaction site.

During the formation of the BSA-ENRO complex, processes of conformational adjustments at the binding site of the protein may occur as ligand interacts. This process is also accompanied by the release of water molecules that are solvating the ligand and the binding site in the protein. The negative values of ΔS° show that the processes of conformational adjustments at the binding site of the proteins are more significant than the release of water molecules from the solvation layer. With increasing temperature the values of ΔS° became less negative, ie, the contribution of water release from the solvation layer increases with increasing temperature.

The negative values of ΔG° indicated that, in the temperature range used in our study, the BSA-ENRO complex was more stable than the free ENRO and BSA molecules in the equilibrium ENRO + BSA ⇌ BSA-ENRO. However, despite the remarkable variation of ΔH° and TΔS° over the temperature the ΔG° values showed a weak variation. Many different thermodynamic processes, such as the interaction between BSA, HSA and tartrazine[90]; BSA, HSA and drugs[91]; BSA and levofloxacin[86], have shown this kind of behavior, known as enthalpy-entropy compensation (EEC). The EEC phenomenon found here (Figure 3) can be described by a reduction on the enthalpy accomplished by a reduction in the entropy.

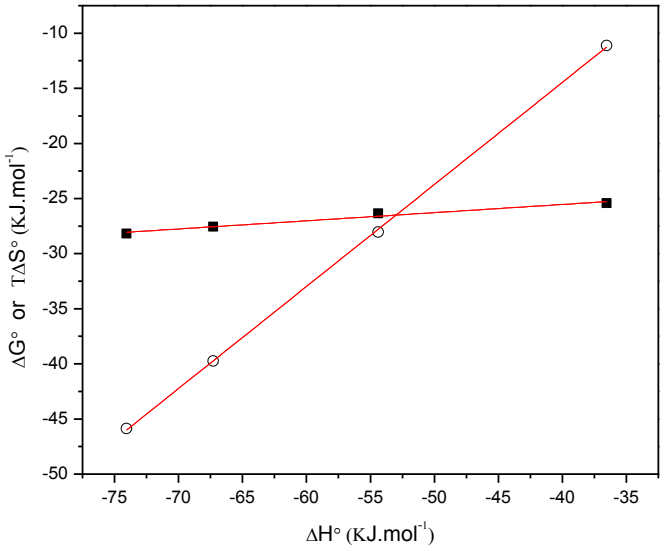

Figure 3: Plots of enthalpy-entropy compensation, (○) TΔS° vs. ΔH° and (■) ΔG° vs. ΔH° for the binding of ENRO to BSA at pH 7.40.

The enthalpy component reflects the amount of thermal energy change associated with binding, while the entropic component quantifies the energy distribution changes between the various quantum levels of the ligand (ENRO), protein (BSA) and the solvent [92,93]. The process of binding in aqueous solution is composed of a series of processes, including the approximation of the ligand in the protein, the desolvation of the ligand and the binding site of the protein, the conformational change of the protein

when the ligand enters its cavity and the solvation of the formed complex. The desolvation process can result in an increase in the entropy of the system as the degree of freedom of the water molecules increases[94,95,96]. However, the binding of the ligand with the protein may result in a decrease in the entropy of both molecules. The enthalpy change may be due to formation and breaking of hydrogen and van der Waals bonds, inducing less or more enthalpy change[96].

These modifications of the thermodynamic parameters may indicate the enthalpy-entropy compensation phenomenon, and can be described as following equation $T\Delta S° = \alpha\ \Delta H° + \beta$. In fact, as shown in figure 3, a linear relationship was obtained according to where the slope and the intercept (α and β) were 0.92 and 22.57, respectively. The slope near of unity suggests that ΔH° are often compensated by corresponding $T\Delta S°$ [97,98,93] that is, the release of energy in the system due to the new interactions formed during the formation of the complex bLF-CUR is compensated by the reduction of the entropy of the system due to the conformational changes in the interaction site. This effect of the enthalpy-entropy compensation for non-covalent bindings can be confirmed by the linearity of the graph of ΔG° versus ΔH° [98,91], indicating almost complete enthalpy-entropy compensation. Thus despite the observed change in ΔH° and ΔS°, Gibbs free energy change remained almost unchanged. The ΔG° values show a narrow range of variation, referring to biological processes involving any non-chemical reversible type of binding[99].

From the dependence of ΔH° values on temperature was possible to determine the standard heat capacity change, ΔCp°, using the relation: $\Delta C_p^o = \left(\frac{\partial H°}{\partial T}\right)_P$.

In Figure 4 it is illustrate the temperature dependence of ΔH° associated with the binding of ENRO to BSA. A linear fit (R^2=0.998) was obtained, and the slope is the measurement of the heat capacity change between the initial and final states of the system. The ΔC_p^o value was 1.24 kJ K^{-1} mol^{-1}.

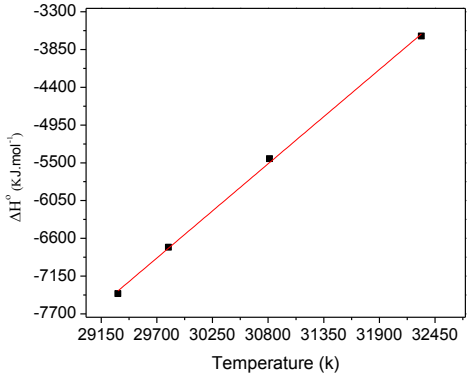

Figure 4: Plot of variation of the standard molar enthalpy change (ΔH°) *versus* temperature for the BSA-ENRO binding.

The ΔC_p^o value is an important thermodynamic parameter that provide useful information about the type and magnitude of the forces governing the binding as well as structural changes of the protein in response to the binding[100,99]. Considering that $\Delta C_p^o = C_{p-complex}^o - (C_{p-BSA}^o + C_{p-ENRO}^o)$, a positive ΔC_p^o indicates that the BSA-ENRO complex has more ability to transfer heat energy to the potential forms than the free BSA and ENRO molecules. This superior capability is due the new intermolecular interactions formed when the complex is formed, that is, the interactions between BSA-ENRO and complex-H_2O dominate the H_2O-H_2O interactions. The negative TΔS° values corroborates this positive ΔC_p^o value, because they suggest that the system entropy decreasing became from the formation of new intermolecular interactions between BSA and ENRO. These new interactions increase the contributions of potential energy for the total system energy.

The value of ΔCp° provides information not only about energy, but also on the structural data and the reorganization of the solvent during complex formation[101]. Thus, the ΔCp° value is also related to the amount of hydrophobic surface area exposed. The positive ΔCp° value indicates the solvation of hydrophobic regions, i.e., after the formation of the complex there was a greater exposure of the apolar regions[102,95,98,103,104], caused by the protein conformational change induced by interactions with ENRO.

4. Conclusions

ENRO showed to bind the BSA at physiological pH, the interaction being reduced with increasing temperature. Probes experiments revealed that ENRO binds preferentially to subdomain IIA (site I) of BSA, containing hydrophobic and positively charged regions. After the thermodynamic study it was found that the fluorescence quenching process was exothermic and that the complex formed is more stable than the free molecules. The formation of the BSA-ENRO complex was a process accompanied by the ECC phenomenon, where the enthalpy increase was compensated by the increase of the entropy. In addition, it was found that the new interactions that occur for complex formation (BSA-ENRO) increase the contributions of potential energy to the total energy of the system, that is, the complex formed (BSA-ENRO) had a greater capacity to transfer energy to the potential forms than the free molecules.

This more detailed thermodynamic study, which reflects theoretical data on the interaction between BSA and ENRO, may be a useful guide in the use of BSA as carrier, providing some important data for the clinical study of the drug, with great significance in clinical medicine.

Acknowledgments

We are gratiful to the Coordenação de Aperfeiçoamento de Pessoal de Nivel Superior – Brasil (CAPES) – Finance Code 001, Conselho Nacional de Desenvolvimento Científico e Tecnológico and Fundação de Amparo à Pesquisa do Estado de Minas Gerais for the financial support.

5. References

(1) Farnaud, S.; Evans, R. W. Lactoferrin - A multifunctional protein with antimicrobial properties. *Mol. Immunol.* **2003**, *40* (7), 395–405.

(2) Steijns, J. M.; van Hooijdonk, A. C. M. Occurrence, structure, biochemical properties and technological characteristics of lactoferrin. *Br. J. Nutr.* **2000**, *84* (S1).

(3) Croguennec, T.; Li, N.; Phelebon, L.; Garnier-Lambrouin, F.; Gésan-Guiziou, G. Interaction between lactoferrin and casein micelles in skimmed milk. *Int. Dairy J.*

2012, *27* (1–2), 34–39.

(4) Darwish, S.; Mozaffari, S.; Parang, K.; Tiwari, R. Cyclic peptide conjugate of curcumin and doxorubicin as an anticancer agent. *Tetrahedron Lett.* **2017**, *58* (49), 4617–4622.

(5) Hussain, Z.; Thu, H. E.; Amjad, M. W.; Hussain, F.; Ahmed, T. A.; Khan, S. Exploring recent developments to improve antioxidant, anti-inflammatory and antimicrobial efficacy of curcumin: A review of new trends and future perspectives. *Mater. Sci. Eng. C* **2017**, *77*, 1316–1326.

(6) Ward, P. P.; Paz, E.; Conneely, O. M. Multifunctional roles of lactoferrin: A critical overview. *Cell. Mol. Life Sci.* **2005**, *62* (22), 2540–2548.

(7) Sreedhara, A.; Flengsrud, R.; Langsrud, T.; Kaul, P.; Prakash, V.; Vegarud, G. E. Structural characteristic, pH and thermal stabilities of apo and holo forms of caprine and bovine lactoferrins. *BioMetals* **2010**, *23* (6), 1159–1170.

(8) Ripolles, D.; Harouna, S.; Parrón, J. A.; Calvo, M.; Pérez, M. D.; Carramiñana, J. J.; Sánchez, L. Antibacterial activity of bovine milk lactoferrin and its hydrolysates prepared with pepsin, chymosin and microbial rennet against foodborne pathogen Listeria monocytogenes. *Int. Dairy J.* **2015**, *45*, 15–22.

(9) Iglesias-Figueroa, B. F.; Espinoza-Sánchez, E. A.; Siqueiros-Cendón, T. S.; Rascón-Cruz, Q. Lactoferrin as a nutraceutical protein from milk, an overview. *Int. Dairy J.* **2019**, *89*, 37–41.

(10) Bokkhim, H.; Bansal, N.; Grøndahl, L.; Bhandari, B. Interactions between different forms of bovine lactoferrin and sodium alginate affect the properties of their mixtures. *Food Hydrocoll.* **2015**, *48*, 38–46.

(11) Wakabayashi, H.; Yamauchi, K.; Takase, M. Lactoferrin research, technology and applications. *Int. Dairy J.* **2006**, *16* (11), 1241–1251.

(12) TOMITA, M.; WAKABAYASHI, H.; SHIN, K.; YAMAUCHI, K.; YAESHIMA, T.; IWATSUKI, K. Twenty-five years of research on bovine lactoferrin applications. *Biochimie* **2009**, *91* (1), 52–57.

(13) Yang, W.; Liu, F.; Xu, C.; Yuan, F.; Gao, Y. Molecular interaction between (-)-epigallocatechin-3-gallate and bovine lactoferrin using multi-spectroscopic method and isothermal titration calorimetry. *Food Res. Int.* **2014**, *64*, 141–149.

(14) Ferraro, V.; Madureira, A. R.; Sarmento, B.; Gomes, A.; Pintado, M. E. Study of the interactions between rosmarinic acid and bovine milk whey protein α-Lactalbumin, β-Lactoglobulin and Lactoferrin. *Food Res. Int.* **2015**, *77*, 450–459.

(15) Jain, B. A spectroscopic study on stability of curcumin as a function of pH in silica nanoformulations, liposome and serum protein. *J. Mol. Struct.* **2017**, *1130*, 194–198.

(16) Stankovic, I. Curcumin. *Joint FAO/WHO Expert Committee on Food Additives*. 2004, pp 1–8.

(17) Bharal, N.; Sahaya, K.; Jain, S.; Mediratta, P. K.; Sharma, K. K. Curcumin has anticonvulsant activity on increasing current electroshock seizures in mice. *Phyther. Res.* **2008**, *22* (12), 1660–1664.

(18) Noratto, G. D.; Jutooru, I.; Safe, S.; Angel-Morales, G.; Mertens-Talcott, S. U. The drug resistance suppression induced by curcuminoids in colon cancer SW-480 cells is mediated by reactive oxygen species-induced disruption of the microRNA-27a-ZBTB10-Sp axis. *Mol. Nutr. Food Res.* **2013**, *57* (9), 1638–1648.

(19) Ying, M.; Huang, F.; Ye, H.; Xu, H.; Shen, L.; Huan, T.; Huang, S.; Xie, J.; Tian, S.; Hu, Z.; et al. Study on interaction between curcumin and pepsin by spectroscopic and docking methods. *Int. J. Biol. Macromol.* **2015**, *79*, 201–208.

(20) Shin, G. H.; Li, J.; Cho, J. H.; Kim, J. T.; Park, H. J. Enhancement of Curcumin Solubility by Phase Change from Crystalline to Amorphous in Cur-TPGS Nanosuspension. *J. Food Sci.* **2016**, *81* (2), N494–N501.

(21) Maiti, K.; Mukherjee, K.; Gantait, A.; Saha, B. P.; Mukherjee, P. K. Curcumin–phospholipid complex: Preparation, therapeutic evaluation and pharmacokinetic study in rats. *Int. J. Pharm.* **2007**, *330* (1–2), 155–163.

(22) Wang, X.; Jiang, Y.; Wang, Y.-W.; Huang, M.-T.; Ho, C.-T.; Huang, Q. Enhancing anti-inflammation activity of curcumin through O/W nanoemulsions. *Food Chem.* **2008**, *108* (2), 419–424.

(23) Ge, Y.-S.; Jin, C.; Song, Z.; Zhang, J.-Q.; Jiang, F.-L.; Liu, Y. Multi-spectroscopic analysis and molecular modeling on the interaction of curcumin and its derivatives with human serum albumin: A comparative study. *Spectrochim. Acta Part A Mol. Biomol. Spectrosc.* **2014**, *124*, 265–276.

(24) Mangolim, C. S.; Moriwaki, C.; Nogueira, A. C.; Sato, F.; Baesso, M. L.; Neto, A. M.; Matioli, G. Curcumin–β-cyclodextrin inclusion complex: Stability, solubility, characterisation by FT-IR, FT-Raman, X-ray diffraction and photoacoustic spectroscopy, and food application. *Food Chem.* **2014**, *153*, 361–370.

(25) Esmaili, M.; Ghaffari, S. M.; Moosavi-Movahedi, Z.; Atri, M. S.; Sharifizadeh, A.; Farhadi, M.; Yousefi, R.; Chobert, J.-M.; Haertlé, T.; Moosavi-Movahedi, A. A. Beta casein-micelle as a nano vehicle for solubility enhancement of curcumin; food industry application. *LWT - Food Sci. Technol.* **2011**, *44* (10), 2166–2172.

(26) Hudson, E. A.; de Paula, H. M. C.; Ferreira, G. M. D.; Ferreira, G. M. D.; Hespanhol, M. do C.; da Silva, L. H. M.; Pires, A. C. dos S. Thermodynamic and kinetic analyses of curcumin and bovine serum albumin binding. *Food Chem.* **2018**, *242*, 505–512.

(27) García-Montoya, I. A.; Cendón, T. S.; Arévalo-Gallegos, S.; Rascón-Cruz, Q. Lactoferrin a multiple bioactive protein: An overview. *Biochim. Biophys. Acta - Gen. Subj.* **2012**, *1820* (3), 226–236.

(28) Sharma, S.; Sinha, M.; Kaushik, S.; Kaur, P.; Singh, T. P. C-lobe of lactoferrin: The whole story of the half-molecule. *Biochem. Res. Int.* **2013**, No. May.

(29) Bollimpelli, V. S.; Kumar, P.; Kumari, S.; Kondapi, A. K. Neuroprotective effect of curcumin-loaded lactoferrin nano particles against rotenone induced neurotoxicity. *Neurochem. Int.* **2016**, *95*, 37–45.

(30) Atrahimovich, D.; Vaya, J.; Tavori, H.; Khatib, S. Glabridin Protects Paraoxonase 1 from Linoleic Acid Hydroperoxide Inhibition via Specific Interaction: A Fluorescence-Quenching Study. *J. Agric. Food Chem.* **2012**, *60* (14), 3679–3685.

(31) Schasfoort, R. B. M.; Tudos, A. J. *Handbook of Surface Plasmon Resonance*; 2013; Vol. 53.

(32) Atale, S. S.; Dyawanapelly, S.; Jagtap, D. D.; Jain, R.; Dandekar, P. Understanding the nano-bio interactions using real-time surface plasmon resonance tool. *Int. J. Biol. Macromol.* **2019**, *123*, 97–107.

(33) Gombau, J.; Nadal, P.; Canela, N.; Gómez-Alonso, S.; García-Romero, E.; Smith, P.; Hermosín-Gutiérrez, I.; Canals, J. M.; Zamora, F. Measurement of the interaction between mucin and oenological tannins by Surface Plasmon Resonance (SPR); relationship with astringency. *Food Chem.* **2019**, *275*, 397–406.

(34) de Paula, H. M. C.; Coelho, Y. L.; Agudelo, A. J. P.; Rezende, J. de P.; Ferreira, G. M. D.; Ferreira, G. M. D.; Pires, A. C. dos S.; da Silva, L. H. M. Kinetics and thermodynamics of bovine serum albumin interactions with Congo red dye.

Colloids Surfaces B Biointerfaces **2017**, *159*, 737–742.

(35) Bi, H.; Tang, L.; Gao, X.; Jia, J.; Lv, H. Spectroscopic analysis on the binding interaction between tetracycline hydrochloride and bovine proteins β-casein, α-lactalbumin. *J. Lumin.* **2016**, *178*, 72–83.

(36) Lakowicz, J. R. *Principles of fluorescence spectroscopy*; 2006.

(37) Silva, M. S.; García-Estévez, I.; Brandão, E.; Mateus, N.; de Freitas, V.; Soares, S. Molecular Interaction Between Salivary Proteins and Food Tannins. *J. Agric. Food Chem.* **2017**, *65* (31), 6415–6424.

(38) Lelis, C. A.; Hudson, E. A.; Ferreira, G. M. D.; Ferreira, G. M. D.; da Silva, L. H. M.; da Silva, M. do C. H.; Pinto, M. S.; Pires, A. C. dos S. Binding thermodynamics of synthetic dye Allura Red with bovine serum albumin. *Food Chem.* **2017**, *217*, 52–58.

(39) Nunes, N. M.; Pacheco, A. F. C.; Agudelo, Á. J. P.; da Silva, L. H. M.; Pinto, M. S.; Hespanhol, M. do C.; Pires, A. C. dos S. Interaction of cinnamic acid and methyl cinnamate with bovine serum albumin: A thermodynamic approach. *Food Chem.* **2017**, *237*, 525–531.

(40) Mohammadi, F.; Moeeni, M. Study on the interactions of trans-resveratrol and curcumin with bovine α-lactalbumin by spectroscopic analysis and molecular docking. *Mater. Sci. Eng. C* **2015**, *50*, 358–366.

(41) Mohammadi, F.; Bordbar, A.-K.; Divsalar, A.; Mohammadi, K.; Saboury, A. A. Interaction of Curcumin and Diacetylcurcumin with the Lipocalin Member β-Lactoglobulin. *Protein J.* **2009**, *28* (3–4), 117–123.

(42) Bolel, P.; Mahapatra, N.; Halder, M. Optical Spectroscopic Exploration of Binding of Cochineal Red A with Two Homologous Serum Albumins. *J. Agric. Food Chem.* **2012**, *60*, 3727–3734.

(43) Patching, S. G. Surface plasmon resonance spectroscopy for characterisation of membrane protein–ligand interactions and its potential for drug discovery. *Biochim. Biophys. Acta - Biomembr.* **2014**, *1838* (1), 43–55.

(44) Ferrante, A.; Gorski, J. Enthalpy-entropy compensation and cooperativity as thermodynamic epiphenomena of structural flexibility in ligand-receptor interactions. *J. Mol. Biol.* **2012**, *417* (5), 454–467.

(45) Bou-Abdallah, F.; Sprague, S. E.; Smith, B. M.; Giffune, T. R. Binding thermodynamics of Diclofenac and Naproxen with human and bovine serum albumins: A calorimetric and spectroscopic study. *J. Chem. Thermodyn.* **2016**, *103*, 299–309.

(46) Niedzwiecka, A.; Stepinski, J.; Darzynkiewicz, E.; Sonenberg, N.; Stolarski, R. Positive Heat Capacity Change upon Specific Binding of Translation Initiation Factor eIF4E to mRNA 5 ‘ Cap Positive Heat Capacity Change upon Specific Binding of Translation Initiation Factor eIF4E to mRNA 5 ′ Cap †. *Biochemistry* **2002**, 12140–12148.

(47) Perozzo, R.; Folkers, G.; Scapozza, L. Thermodynamics of protein-ligand interactions: History, presence, and future aspects. *J. Recept. Signal Transduct.* **2004**, *24* (1–2), 1–52.

(48) Smith, I. W. M. The temperature-dependence of elementary reaction rates: beyond Arrhenius. *Chem. Soc. Rev.* **2008**, *37* (4), 812–826.

(49) Pan, A.; Biswas, T.; Rakshit, A. K.; Moulik, S. P. Enthalpy–Entropy Compensation (EEC) Effect: A Revisit. *J. Phys. Chem. B* **2015**, *119* (52), 15876–15884.

(50) Cheng, L.-Y.; Xia, W.; Zhang, X.; Bai, A.-M.; Ouyang, Y.; Hu, Y.-J. In vitro binding comparison of cephalosporins to human serum albumin by spectroscopy

and molecular docking approaches: A novel structural pursuing. *J. Mol. Liq.* **2017**, *248*, 168–176.

(51) KuKanich, B.; Gehring, R.; Webb, A. I.; Craigmill, A. L.; Riviere, J. E. Effect of formulation and route of administration on tissue residues and withdrawal times. *J. Am. Vet. Med. Assoc.* **2005**, *227* (10), 1574–1577.

(52) Martins, M. T.; Barreto, F.; Hoff, R. B.; Jank, L.; Arsand, J. B.; Motta, T. M. C.; Schapoval, E. E. S. Multiclass and multi-residue determination of antibiotics in bovine milk by liquid chromatography–tandem mass spectrometry: Combining efficiency of milk control and simplicity of routine analysis. *Int. Dairy J.* **2016**, *59*, 44–51.

(53) BROWN, S. A. Fluoroquinolones in animal health. *J. Vet. Pharmacol. Ther.* **1996**, *19* (1), 1–14.

(54) Attili, A. R.; Preziuso, S.; Ngu Ngwa, V.; Cantalamessa, A.; Moriconi, M.; Cuteri, V. Clinical evaluation of the use of enrofloxacin against Staphylococcus aureus clinical mastitis in sheep. *Small Rumin. Res.* **2016**, *136*, 72–77.

(55) Giguère, S.; Dowling, P. M. Fluoroquinolones. In *Antimicrobial Therapy in Veterinary Medicine*; John Wiley & Sons, Inc: Hoboken, NJ, 2013; pp 295–314.

(56) Idowu, O. R.; Peggins, J. O.; Cullison, R.; Bredow, J. von. Comparative pharmacokinetics of enrofloxacin and ciprofloxacin in lactating dairy cows and beef steers following intravenous administration of enrofloxacin. *Res. Vet. Sci.* **2010**, *89* (2), 230–235.

(57) Liu, Z.; Chan, L.; Ye, X.; Bai, Y.; Chen, T. BSA-Based Cu 2 Se Nanoparticles with Multistimuli-Responsive Drug Vehicles for Synergistic Chemo-Photothermal Therapy. *Colloids Surfaces B Biointerfaces* **2018**.

(58) Salehiabar, M.; Nosrati, H.; Javani, E.; Aliakbarzadeh, F.; Kheiri Manjili, H.; Davaran, S.; Danafar, H. Production of biological nanoparticles from bovine serum albumin as controlled release carrier for curcumin delivery. *Int. J. Biol. Macromol.* **2018**, *115*, 83–89.

(59) McCann, D.; Barrett, A.; Cooper, A.; Crumpler, D.; Dalen, L.; Grimshaw, K.; Kitchin, E.; Lok, K.; Porteous, L.; Prince, E.; et al. Food additives and hyperactive behaviour in 3-year-old and 8/9-year-old children in the community: a randomised, double-blinded, placebo-controlled trial. *Lancet* **2007**, *370* (9598), 1560–1567.

(60) Lin, Y.; Jiao, G.; Sun, G.; Zhang, L.; Wang, S.; Liu, H.; Li, Z. Binding of teicoplanin and vancomycin to bovine serum albumin in vitro: A multispectroscopic approach and molecular modeling. *Luminescence* **2014**, *29* (2), 109–117.

(61) Jattinagoudar, L.; Meti, M.; Nandibewoor, S.; Chimatadar, S. Evaluation of the binding interaction between bovine serum albumin and dimethyl fumarate, an anti-inflammatory drug by multispectroscopic methods. *Spectrochim. Acta - Part A Mol. Biomol. Spectrosc.* **2016**, *156*, 164–171.

(62) Guo, M.; Lu, W.-J.; Yi, P.-G.; Yu, Q.-S. Study on the thermodynamic characteristics between fluoroquinolone and bovine serum albumin. *J. Chem. Thermodyn.* **2007**, *39* (3), 337–343.

(63) Seedher, N.; Agarwal, P. Complexation of fluoroquinolone antibiotics with human serum albumin: A fluorescence quenching study. *J. Lumin.* **2010**, *130* (10), 1841–1848.

(64) Liu, B.; Xue, C.; Wang, J.; Yang, C.; Lv, Y. Study of the quenching mechanism of bovine serum albumin with presence of chloramphenicol and enrofloxacin. *Phys. Chem.* **2011**, *6* (2).

(65) Ni, Y.; Su, S.; Kokot, S. Spectrometric studies on the interaction of fluoroquinolones and bovine serum albumin. *Spectrochim. Acta - Part A Mol. Biomol. Spectrosc.* **2010**, *75* (2), 547–552.

(66) Reddy, T. K.; Srikanth, G.; Mallikarjun, V.; Nivethithai, P. MECHANISM OF INTERACTION OF SOME ANTIMICROBIAL AGENTS WITH BOVINE SERUM ALBUMIN. *J. Glob. Pharma Technol.* **2009**, *2* (March 2010), 47–55.

(67) Qin, P.; Pan, X.; Liu, R.; Hu, C.; Dong, Y. Toxic interaction mechanism of two fluoroquinolones with serum albumin by spectroscopic and computational methods. *J. Environ. Sci. Heal. - Part B Pestic. Food Contam. Agric. Wastes* **2017**, *52* (11), 833–841.

(68) Wang, L.; Zhang, G.; Wang, Y. Binding properties of food colorant allura red with human serum albumin in vitro. *Mol. Biol. Rep.* **2014**, *41* (5), 3381–3391.

(69) Ma, L.; Liu, B.; Wang, C.; Zhang, H.; Cheng, X. The Investigation of Fluorescence Spectra and Fluorescence Quantum Yield of Enrofloxacin. **2018**, *2* (1), 11–16.

(70) Lizondo, M.; Pons, M.; Gallardo, M.; Estelrich, J. Physicochemical properties of enrofloxacin. *J. Pharm. Biomed. Anal.* **1997**, *15* (12), 1845–1849.

(71) Bi, S.; Song, D.; Tian, Y.; Zhou, X.; Liu, Z.; Zhang, H. Molecular spectroscopic study on the interaction of tetracyclines with serum albumins. *Spectrochim. Acta - Part A Mol. Biomol. Spectrosc.* **2005**, *61* (4), 629–636.

(72) Schneider, M. J. Rapid Fluorescence Screening Assay for Enrofloxacin and Tetracyclines in Chicken Muscle. *J. Agric. Food Chem.* **2004**, *52* (26), 7809–7813.

(73) Yazdi, S. R.; Corredig, M. Heating of milk alters the binding of curcumin to casein micelles . A fluorescence spectroscopy study. *Food Chem.* **2012**, *132* (3), 1143–1149.

(74) Benesi, H. A.; Hildebrand, J. H. a Spectrophotometric Investigation of the Interaction of Iodine With Aromatic Hydrocarbons. *J. Am. Chem. Soc.* **1949**, *71* (8), 2703–2707.

(75) Bensouilah, N.; Abdaoui, M. Inclusion complex of N-nitroso, N-(2-chloroethyl), N`, N`-dibenzylsulfamid with β-Cyclodextrin: Fluorescence and molecular modeling. *Comptes Rendus Chim.* **2012**, *15* (11–12), 1022–1036.

(76) Otagiri, M. A Molecular Functional Study on the Interactions of Drugs with Plasma Proteins. *Drug Metab. Pharmacokinet.* **2005**, *20* (5), 309–323.

(77) Roy, S. Review on Interaction of Serum Albumin with Drug Molecules. *Res. Rev. J. Pharmacol. Toxicol. Stud.* **2016**, *4* (2), 1–10.

(78) Ming Guo, Wei-Jun Lu, Ping-Gui Yi, Q.-S. Y. Study on the thermodynamic characteristics between fluoroquinolone and bovine serum albumin. *J. Chem. Thermodyn.* **2007**, *39*, 337–343.

(79) Sinisi, V.; Forzato, C.; Cefarin, N.; Navarini, L.; Berti, F. Interaction of chlorogenic acids and quinides from coffee with human serum albumin. *FOOD Chem.* **2015**, *168*, 332–340.

(80) Bourassa, P.; Kanakis, C. D.; Tarantilis, P.; Pollissiou, M. G.; Tajmir-Riahi, H. a. Resveratrol, genistein, and curcumin bind bovine serum albumin. *J. Phys. Chem. B* **2010**, *114* (9), 3348–3354.

(81) Pal, U.; Pramanik, S. K.; Bhattacharya, B.; Banerji, B.; Maiti, N. C. Binding interaction of a novel fluorophore with serum albumins: steady state fluorescence perturbation and molecular modeling analysis. *Springerplus* **2015**, *4* (1).

(82) Li, M.; Hagerman, A. E. Role of the Flavan-3-ol and Galloyl Moieties in the Interaction of (−)-Epigallocatechin Gallate with Serum Albumin. *J. Agric. Food Chem.* **2014**, *62* (17), 3768–3775.

(83) Datta, S.; Mahapatra, N.; Halder, M. pH-insensitive electrostatic interaction of carmoisine with two serum proteins: A possible caution on its uses in food and pharmaceutical industry. *J. Photochem. Photobiol. B Biol.* **2013**, *124*, 50–62.

(84) Majorek, K. A.; Porebski, P. J.; Dayal, A.; Zimmerman, M. D.; Jablonska, K.; Stewart, A. J.; Chruszcz, M.; Minor, W. Structural and immunologic characterization of bovine, horse, and rabbit serum albumins. *Mol. Immunol.* **2012**, *52* (3–4), 174–182.

(85) Khatun, S.; Riyazuddeen; Yasmeen, S.; Kumar, A.; Subbarao, N. Calorimetric, spectroscopic and molecular modelling insight into the interaction of gallic acid with bovine serum albumin. *J. Chem. Thermodyn.* **2018**, *122*, 85–94.

(86) Kaur, A.; Khan, I. A.; Banipal, P. K.; Banipal, T. S. Deciphering the complexation process of a fluoroquinolone antibiotic, levofloxacin, with bovine serum albumin in the presence of additives. *Spectrochim. Acta - Part A Mol. Biomol. Spectrosc.* **2018**, *191*, 259–270.

(87) Yuan, J.-L.; Iv, Z.; Liu, Z.-G.; Hu, Z.; Zou, G.-L. Study on interaction between apigenin and human serum albumin by spectroscopy and molecular modeling. *J. Photochem. Photobiol. A Chem.* **2007**, *191* (2–3), 104–113.

(88) Ross, P. D.; Subramanian, S. Thermodynamics of protein association reactions: forces contributing to stability. *Biochemistry* **1981**, *20* (11), 3096–3102.

(89) Cui, F.-L.; Wang, J.-L.; Cui, Y.-R.; Li, J.-P. Fluorescent investigation of the interactions between N-(p-chlorophenyl)-N′-(1-naphthyl) thiourea and serum albumin: Synchronous fluorescence determination of serum albumin. *Anal. Chim. Acta* **2006**, *571* (2), 175–183.

(90) Basu, A.; Kumar, G. S. Thermodynamics of the interaction of the food additive tartrazine with serum albumins: a microcalorimetric investigation. *Food Chem.* **2015**, *175*, 137–142.

(91) Bou-Abdallah, F.; Sprague, S. E.; Smith, B. M.; Giffune, T. R. Binding thermodynamics of Diclofenac and Naproxen with human and bovine serum albumins: A calorimetric and spectroscopic study. *J. Chem. Thermodyn.* **2016**, *103*, 299–309.

(92) Chaires, J. B. Calorimetry and Thermodynamics in Drug Design. *Annu. Rev. Biophys.* **2008**, *37* (1), 135–151.

(93) Chodera, J. D.; Mobley, D. L. Entropy-enthalpy compensation: Role and ramifications in biomolecular ligand recognition and design. *Annu Rev Biophys* **2014**, *42*, 121–142.

(94) Sturtevant, J. M. Heat capacity and entropy changes in processes involving proteins. *Proc. Natl. Acad. Sci.* **1977**, *74* (6), 2236–2240.

(95) Perozzo, R.; Folkers, G.; Scapozza, L. Thermodynamics of protein-ligand interactions: history, presence, and future aspects. *J. Recept. Signal Transduct. Res.* **2004**, *24* (1–2), 1–52.

(96) Saini, R. D. Thermodynamics of protein-ligand interactions and their analysis. *J. Proteins Proteomics* **2017**, *8* (4), 205–217.

(97) Ford, D. M. Enthalpy−Entropy Compensation is Not a General Feature of Weak Association. *J. Am. Chem. Soc.* **2005**, *127* (46), 16167–16170.

(98) Ball, V.; Maechling, C. Isothermal microcalorimetry to investigate non specific interactions in biophysical chemistry. *Int. J. Mol. Sci.* **2009**, *10* (8), 3283–3315.

(99) Molina-Bolívar, J. A.; Ruiz, C. C.; Galisteo-González, F.; O'Donnell, M. M.; Parra, A. Energetics of albumin-disuccinylmaslinic acid binding determined by fluorescence spectroscopy. *Fluid Phase Equilib.* **2015**, *400*, 43–52.

(100) Banerjee, T.; Singh, S. K.; Kishore, N. Binding of Naproxen and Amitriptyline to Bovine Serum Albumin: Biophysical Aspects. *J. Phys. Chem. B* **2006**, *110* (47), 24147–24156.

(101) Xu, Y.; Oruganti, S. V.; Gopalan, V.; Foster, M. P. Thermodynamics of coupled folding in the interaction of archaeal RNase P proteins RPP21 and RPP29. *Biochemistry* **2012**, *51* (4), 926–935.

(102) Spolar, R.; Record, M. Coupling of local folding to site-specific binding of proteins to DNA. *Science (80-.).* **1994**, *263* (5148), 777–784.

(103) Banipal, T. S.; Kaur, N.; Banipal, P. K. Binding studies of caffeine and theophylline to bovine serum albumin: Calorimetric and spectroscopic approach. *J. Mol. Liq.* **2016**, *223*, 1048–1055.

(104) Vega, S.; Abian, O.; Velazquez-Campoy, A. On the link between conformational changes, ligand binding and heat capacity. *Biochim. Biophys. Acta - Gen. Subj.* **2016**, *1860* (5), 868–878.

CONCLUÇÃO GERAL

Proteínas do leite como BSA e lactoferrina demonstraram interagir com compostos de interesse na área de alimentos. Por espectroscopia de florescência foi possível verificar que lactoferrina interage com curcumina por meio de interações hidrofóbicas apresentando potencial para veicular um número significativo de curcumina. A determinação da constante de interação obtidas por espectroscopia de fluorescência e por ressonância plasmônica de superfície sugeriu que as interação que ocorrem nos sítios distantes dos resíduos de triptofano são mais fracas e acompanhadas de mudanças conformacionais nos sítios. Os parâmetros termodinâmicos e cinéticos determinados nesse estudo foram influenciados pela temperatura, sendo verificado o ocorrência do fenômeno de compensação entalpica-entropica. Através do estudo cinético também foi possível sugerir que nas baixas temperaturas estudadas a CUR interage na superfície na proteína, já em temperaturas mais elevadas o composto bioativo interage preferencialmente no interior da proteína.

No estudo de interação entre BSA e ENRO foi utilizado a capacidade da enrofloxacina de emitir fluorescência, sendo portanto um estudo baseado em uma propriedade do ligante. Por espectroscopia fluorescência a ENRO demonstrou se ligar preferencialmente ao sitio I da BSA, em pH fisiológico. O processo de interação foi influenciado pela variação de temperatura, sendo também verificado a ocorrência do fenômeno de compensação entalpia-entropia, onde a diminuição da entalpia com o aumento da temperatura foi compensado pelo aumento da entropia.

Assim, o estudo realizado pode ser útil, em futuras aplicações das proteínas do leite como estruturas de transporte para diversas moléculas.